IEEE Access
Multidisciplinary | Rapid Review | Open Access Journal

Received 19 February 2024, accepted 16 March 2024, date of publication 25 March 2024, date of current version 3 April 2024.

Digital Object Identifier 10.1109/ACCESS.2024.3381520

RESEARCH ARTICLE

Data Traffic Based Shape Independent Adaptive Unequal Clustering for Heterogeneous Wireless Sensor Networks

TAMOOR SHAFIQUE, ABDEL-HAMID SOLIMAN, AND ANAS AMJAD
School of Digital, Technology, Innovation and Business, Staffordshire University, ST4 2DE Stoke-on-Trent, U.K.

Corresponding author: Tamoor Shafique (Tamoor.shafique@staffs.ac.uk)

This work was supported by Staffordshire University.

ABSTRACT Due to the technological advancements in wireless communication and their continuously increasing applications in collaborative and cooperative smart infrastructures, energy efficient data collection using wireless devices, has gained significant importance recently. Modern wireless sensor networks refer to network of low-powered and energy-constrained Internet of Things (IoT) devices. Although data collection using hierarchical routing with clustered network improves energy efficiency but introduces energy holes in the region closer to the data gathering center due to heavy relaying load on cluster heads. In this paper, first an improved data gathering center deployment technique for heterogeneous networks has been proposed. Technique for Order of Preference by Similarity to Ideal Solutions (TOPSIS), a multi-criteria decision-making technique, is used to determine the optimal location for the deployment of data gathering center. The proposed technique is adaptive to various shaped networks as required by IoT and increases energy efficiency. Secondly, an unequal clustering based on transmission distances has been proposed. Moreover, cubical, and spherical segmentation schemes for 3D heterogeneous networks have been proposed that assist the formation of unequal clusters. Finally, a shape independent data rate-based segmentation has been proposed that further extends the adaptability and scalability of the proposed unequal clustering. The results demonstrate that the proposed data traffic-based shape independent adaptive clustering scheme increases network lifetime up to 14.2% and 18.8% as compared to Fuzzy Logic based unequal clustering and IUCR respectively. It also reduces the overall network energy consumption up to 61.4% as compared to the state-of-the art unequal clustering methods.

INDEX TERMS Balanced energy routing, energy holes, Internet of Things, shape independent clustering, Scalable clustering protocol, unequal clustering, 3D wireless sensor network.

I. INTRODUCTION

Wireless sensor network (WSN) with the help of Internet of Things (IoT), allows accessibility of sensor data to be used for cooperative and collaborative operations with minimum human intervention. It is a smart self-organizing network of low-power sensor nodes that can inform about the events and changes in environment and can also perform data sensing, storage, processing and wireless communication for IoT applications [1], [2]. With the advancements in microelectromechanical devices and communication technologies not only people but things can communicate anytime, with anything and anyone using any network and service [3]. Wireless sensors are a critical component of IoT systems and allow such systems to perform informed operations and in a flexible manner. An important role of wireless sensors is the transmission of the sensed data to a base station (BS). Hierarchical routing using clustering of wireless sensor nodes has been proven to be energy efficient method for transmission of sensed information.

Due to the increasing applications of IoT in modern interconnected smart cities, the number of IoT devices is

The associate editor coordinating the review of this manuscript and approving it for publication was Md. Abdur Razzaque.

increasing day by day. According to Ericson's forecasts, this number will reach 5.5 B by 2027 [4]. With a growing number of devices, there are challenges of increased energy consumption in the transmission and storage of this huge data. International Data Corporation (IDC) forecasts that IoT connected devices are anticipated to contribute 79.4 ZB towards overall data in 2025 [5]. Moreover, with the steady increase in the global population, that is currently projected to reach almost 10 billion by 2050, there is an intuitive need for energy supply to align with the demand [6].

Generally, clustering of the devices and hierarchical routing is used for energy efficient data collection from these low-powered devices. However, hierarchical routing uses multi-hop communication between cluster heads which implies heavy relaying load on the nearest cluster heads to data gathering center. This results in early energy depletion of the cluster heads closer to data gathering center due to excessive transmission load and introduces energy holes. Several energy hole mitigating techniques have been proposed by authors in [7], [8], [9], [10], [11], [12], [13], [14], [15], [16], [17], [18], [19], [20], [21], [22], [23], [24], [25], [26], [27], [28], [29], [30], [31], [32], [33], [34], [35], [36], [37], [38], [39], [40], [41], [42], [43], [44], [45], [46], [47], [48], and [49]. However, most of these techniques are designed for 2D planar networks [7], [9], [11], [19], [22], [34]. Whereas most of real-life applications of wirelessly connected devices are 3D, such as marine pollution monitoring, multi-floor building data collection and forecast disaster prevention [50]. Moreover, the energy hole mitigating techniques found in literature are network shape specific [11], [16], [19], [24], [25], [38] and have limitations in terms of adaptability, scalability, and flexibility in operation.

To overcome these limitations according to the above-mentioned quality of service (QoS) criterion, this work has the following contributions:

1. Two algorithms for the optimal deployment of data gathering center have been proposed. The proposed algorithms utilize heterogeneous device characteristics such as initial energies, data rates, and locations etc., to determine an energy efficient location of data gathering center. The first algorithm uses an iterative approach to calculate energy consumption of each location whereas the second algorithm uses a multi-criterion decision-making technique TOPSIS, to evaluate alternative locations within the network. The location with best rank output is then selected as optimal location of the data gathering center.
2. Two scalable segmentation techniques have been proposed for 3D cubical and spherical shape heterogeneous networks. These segmentation techniques are designed to determine the distribution of heterogeneous characteristics across different regions of the network. These techniques are then used to produce unequal clusters of devices across the network considering their resources and distances from the data gathering center. Finally, a centroid based calculation for the choice of cluster head in the unequal clusters is determined.
3. To enhance the adaptivity, scalability and flexibility of the fixed shape unequal clustering techniques, a shape independent network segmentation technique has been developed. This technique divides the network into regions of equal data rate and forms unequal clusters of devices by calculating number of cluster heads in a region according to its distance from data gathering center. In addition, a balanced network operation and increased network lifetime has been achieved with this design.
4. A unified clustering and routing method has been proposed that is adaptive, scalable and energy efficient for large scale networks of heterogeneous devices. This method incorporates the computation of a suitable next hop for inter cluster multi-hop communication.

The rest of this paper is organized as follows: Section II introduces related works in energy efficient WSN routing protocols. In section III, the various deployment techniques of data gathering center are evaluated in comparison to proposed optimal deployment of DGC. Section IV presents the main design criteria for proposed cubical and spherical segmentation based unequal clustering. In section V a shape independent adaptive network segmentation scheme has been proposed. Section VI examines the network and radio models. Section VII explains simulation results in terms of DGC deployment, scalability and adaptability, balanced energy operation and increased lifetime of the network. Finally, a conclusion and future work has been described in section VIII.

II. RELATED WORK

Effective utilization of the limited energy resources on devices in WSN assisted IoT is an important and contemporary goal. This goal can be achieved either by using lightweight communication protocols or by limiting energy consumption within devices [51]. The devices consume energy in sensing, processing, storing, transmission, and reception operations. The dominant consumer of energy is the network node's radio operations [52], [53]. Recent techniques to limit energy consumption in radio operations can be classified as: improved transceiver circuit design, transmission power control, cognitive radios and energy-efficient routing [54]. Energy-efficient topology and routing methods have proven to be an emerging area for WSN energy management. Although some applications use flat routing, but hierarchical routing is more promising due to advantages such as increased lifetime, low end-to-end delay and scalability of operation [55]. A disadvantage of hierarchical routing is imbalance between the energy consumption of individual devices due to different roles. Cluster heads consume more energy as compared to normal devices. A significant rationale of initial energy, approximately 90% is still unused when network lifetime is over [56]. Stability and efficient

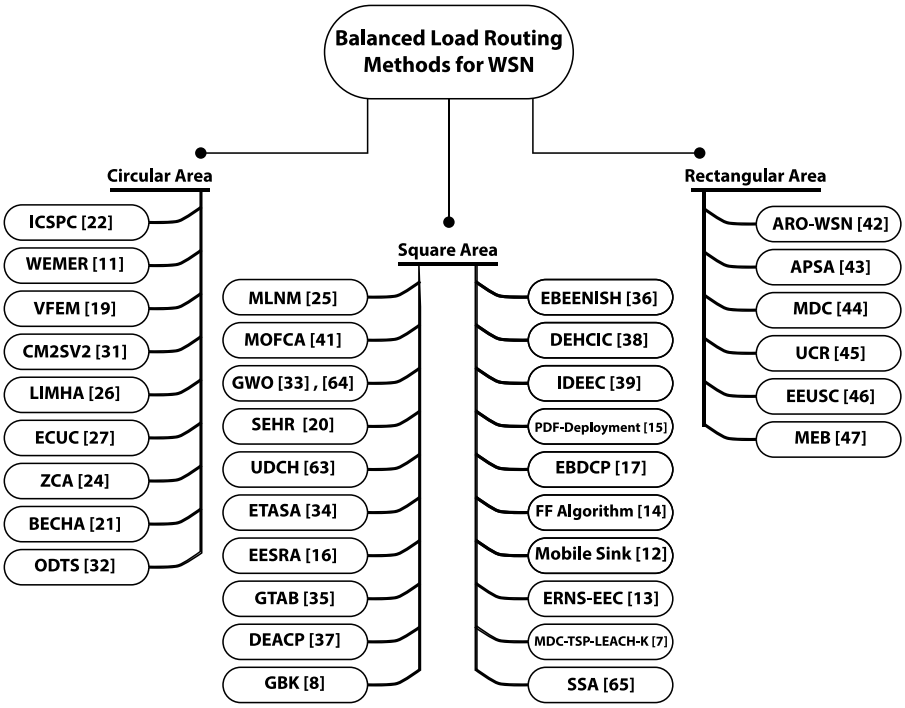

FIGURE 1. Classification of energy hole mitigating methods based on network shape considered.

utilization of energy in network operation is achieved by minimizing time duration between the death of first and last node [57].

Low Energy Adaptive Clustering Hierarchy (LEACH) [58] is a prominent protocol due to rotation of cluster head role between network nodes. However, randomized selection of cluster heads, and consideration of homogeneous devices limit LEACH from achieving best performance. Attempts have been made in LEACH Centralized (LEACH-C) [59] and Hybrid Energy-Efficient Distributed (HEED) [60] clustering to improve the performance. However, these methods use huge number of cluster heads and are suitable only for small scale networks. Cluster-Chain Mobile Agent Routing (CCMAR) [10] improves the energy efficiency by combining advantages of LEACH [58] and Power Efficient Energy Gathering Sensor Information Systems PEGASIS [61]. Wireless Sensor Network Energy Hole Alleviating (WSNEHA) algorithm [40] uses adaptive transceiver range adjustment strategy to enhance network lifetime. To extend the WSNEHA algorithm, authors in [18] proposed a Balanced Energy Consuming and Hole Alleviating (BECHA) algorithm, that balances the load distribution of the entire network. A further improvement of BECHA is Energy Aware BECHA (EA-BECHA), which was proposed later in [21], to reduce the packet drop and further increase the energy efficiency. These efforts do not address end-to-end delay and are not adaptable to varying requirements of WSN assisted IoT. Balanced Energy Adaptive Routing (BEAR) [23] is another similar attempt that only focuses on a specific network shape.

Due to numerous applications of WSN assisted IoT a scalable, and adaptive energy efficient routing scheme is required. Most of existing methods that increase network lifetime and stability are network shape specific. The operation of these methods is also limited to only two-dimensional networks. Whereas most of the real-life applications of sensing devices are 3D. Taxonomy in Figure 1 shows classification of the balanced energy routing techniques with respect to the network shape considered. These techniques use principles of divide and rule. Divide and rule assist in breaking network into smaller segments, network attributes in smaller segments are used to devise balanced routing mechanism. For varying shape and multidimensional network requirements in WSN assisted IoT existing methods have limitations in terms of scalability, and adaptability.

A range of balanced energy routing techniques for two-dimensional circular area have been developed [10], [11], [18], [21], [40], [59], [60], [61], [62]. WEMER [11] is a recent balanced energy routing method suitable for a circular network. It segments the network into circular coronas. Based on the transmission distance each corona segment computes unequal clusters. Soon as the node's energies in a sector reduces below a given threshold, wedges of corresponding sector merge with the nearby sector to increase candidate nodes for cluster head role. Authors in [19] proposed a Virtual Force-Based Energy Hole Mitigating (VFEM) method and divided network into annulus. Relay nodes in each annulus have been deployed. Another method to balance load in a circular area network is Immune Clone Selection-Based Power Control (ICSPC) [22]. It is suitable

for large scale circular networks and reduces energy holes but at the expense of decreased overall network lifetime. Energy Efficient and Coverage Guaranteed Unequal-Sized Clustering (ECUC) [27] computes optimal cluster range and assigns cluster head role to a node near the centroid in the cluster but angle of sectors is fixed and static in nature. Authors in [26] proposed forwarder nodes in a corona-based segmentation but two-level heterogeneity i.e., normal nodes and super nodes, has been exploited to gain network lifetime. A two-stage genetic algorithm has been employed to determine optimal interval of cluster size in Circular Motion of Mobile-Sink with Varied Velocity algorithm (CM2SV2) [31]. Several mobile sinks have been used for the data collection at a single stationary data gathering center. Authors in [24] proposed zonal clustering algorithm with geo-cluster heads. Primary cluster heads are supported with one or more assisting cluster heads. Balanced Energy Consuming and Hole-Alleviating Algorithm (BECHA) [21] does not use clustering but multi-hop communication between nodes at several corona segments and reduces holes. An Optimal Distance Based Transmission Strategy (ODTS) [32] divides the circular network area into disjoint concentric coronas and uses ant colony optimization to balance load with the transmission distance.

Since WSN applications are not limited to circular area a lot of work has also been carried out to increase network lifetime of square area Wireless Networks [12], [13], [14], [15], [16], [17], [20], [25], [33], [34], [35], [36], [37], [38], [39], [63]. A multi-layer network mode [25] shows scalability with both random and controlled deployment of devices. It does not use multi-hop communication between clusters and is unsuitable for large-scale networks.

Multi-Objective Fuzzy Clustering Algorithm (MOFCA) uses fuzzy logic and multi mobile sinks to balance energy consumption in network nodes [41]. Grey Wolf Optimization (GWO) [33], [64] chooses cluster heads by calculating fitness function based on residual energy and distance from the base station. Modified Salp Swarm Algorithm (SSA) has been used in [65] to perform clustering and routing functions in a centralized manner. Three tier communication architecture has been used in Sector-based Energy Hole Reduction (SEHR) [20] to balance load among network nodes in a square field. However, it uses controlled deployment of homogeneous nodes to achieve better performance. Energy and Traffic Aware Sleep-Awake (ETASA) [34] reduces redundancy and balances load but uses penalty to nodes with different energies. Three-layer hierarchy has been proposed in Energy-Efficient Scalable Routing Algorithm (EESRA) [16] that improves the quality of service of square network with homogeneous and stationary nodes. However, extra assistant nodes have been deployed to achieve gain in energy consumption. This introduces high latency in data collection. In Game Theoretic Approach for Balancing (GTAB) [35] an integrated solution with energy harvesting has been proposed. Although it considers heterogeneous nodes, but high energy nodes are penalized. Limited network size is also a disadvantage of this method. Enhanced Energy Efficient Network Integrated Super Heterogeneous (EBEENISH) [36] allows up to four levels of energy heterogeneity among network nodes but network delay due to high complexity of algorithm, jitter and only single hop communication considered makes it unsuitable for large-scale applications. Authors in [37] proposed Distributed Efficient Adaptive Clustering Protocol (DEACP) that gathers data with a load balancing advantage but only considers homogeneous nodes without calculation of optimal number of nodes. Improved Distributed Energy Efficient Clustering (IDEEC) [39] also uses advance and super nodes as second and third level of heterogeneity.

A computational intelligence based worked deployment scheme of [15] increases coverage and reduces energy holes by using controlled deployment of homogeneous nodes. Energy Balanced Distributed Clustering Protocol (EBDCP) [17] is another energy balancing approach for square area network and achieves reduced latency for static homogeneous deployment. The disadvantage is added latency due to mobile sink and energy spent on mobile sink. Authors in [14] divide the network area into equal cells; firefly algorithm is used for scheduling of nodes in area with desired sufficient coverage. It considers both static and mobile homogeneous energy nodes in a square area. To reduce latency mobile sink with 4 or 8 sojourn location path patterns have been proposed in [12]. Additional nodes with relaying function are chosen in [13] and are termed as RN. The scheme initially allows 10 fixed clusters and then dynamically works cluster numbers. Recently researchers in [7] proposed a new hybrid protocol Mobile Data Collectors-Travelling Salesman Problem-Low Energy Adaptive Hierarchy-K-Means (MDC-TSP-LEACH-K). This protocol used grid and k-means algorithm to minimize energy consumption in CH election phase. Furthermore, it used Mobile Data Collector (MDC) as an intermediary between CH and base station to enhance QoS of large-scale networks. It reduced latency by controlling speed of mobile data collector and extended network lifetime. Another grid based clustered routing research in [8] proposed Grid-Based K-means (GBK) clustering and Grid-Based K-means clustering with node scoring mechanism (GBK-R). These efforts although provide good results but pose limitations in terms of scalability and adaptability of operation. Moreover, most of methods are considered to be limited to homogeneous device deployment.

Wireless Sensor Networks have increasing applications in linear or rectangular area networks for example applications in agriculture, railway, and utility supply networks. Balanced operation of network devices is also important in rectangular shape networks to achieve energy efficiency and increased network lifetime. Appropriate Rank-Order Wireless Sensor Networks (ARO-WSN) [42] is a combined hierarchical and distance-based clustering method. Another method that used balanced operation of network nodes in a rectangular shape is Affinity Based Self-Adaptive (APSA) clustering

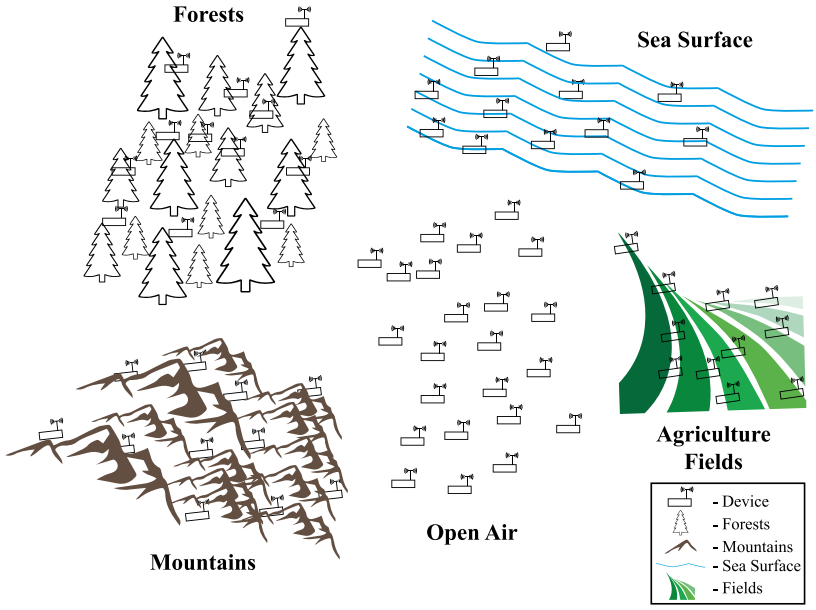

FIGURE 2. Heterogeneous devices deployed in network with varying terrains/shapes.

method [43]. This method uses k-medoids with affinity propagation to increase network lifetime. APSA is limited in terms of scalability and is suitable for homogeneous networks only. A Mobile Data Collector (MDC) [44] uses adjustable transmission range for sensor nodes to increase network lifetime. An optimal speed of mobile data collector has been calculated but latency is high and adaptability to heterogeneous networks has not been considered. Authors in [45] proposed an unequal clustering-based routing for homogeneous nodes in a large-scale rectangular network. Energy Efficient Unequal Sector Clustering (EEUSC) [46] divides the network into multiple sectors with a single base station and balances energy consumption but at the cost of overall network lifetime. Multi energy balancing approach achieved good results by calculating distance to traffic load ratios of each device [47]. This was due to removal of extra overhead.

Most of the above methods consider two-dimensional network structure and utilize shape specific network parameters. This limits the adaptability of these methods in multiple applications. Due to the requirements of flexibility and interoperability in a 3D network of heterogeneous devices such as IoT, existing methods do not perform well. This work addresses the challenges of limited scalability, adaptability, and flexibility in energy efficient hierarchical routing methods. The proposed work also enhances network lifetime and improves network stability.

III. SINK NODE DEPLOYMENT

Due to the increasing applications of WSN assisted IoT, scalability and adaptivity of the energy efficient hierarchical routing methods are important quality of service criterions [54]. Typically, sensing devices are deployed arbitrarily or in a pre-planned manner in a region of interest [19]. However, non-uniform deployment methods [66] result in stable and energy efficient network operation. This is as a result of the increase in number of sensing devices in a geometric progression from outer to inner fragment of the network [67].

In addition to 2D, 3D deployment of microelectromechanical devices is used in applications such as sea surfaces, mountains, smart farming, and precision agriculture [46] as shown in Figure 2. Such applications have varying surface terrains for devices to be deployed and are sometimes located in remote areas. Therefore, controlled deployment is not always achievable and is unrealistic.

Moreover, heterogeneous devices are deployed at various locations in three-dimensional space to serve multiple applications. For an energy efficient data collection, the transceivers are shared between these devices. Although many approaches have been developed for energy efficient data collection in such networks, there is no distinct mechanism for choosing the optimal location of base station [68]. Consequently, most of the network topology approaches locate base station either in the center or at boundary of the region of interest [69].

Therefore, instead of assuming a complete control over device deployment, it is more realistic to determine a suitable location for data gathering center (DGC) in densely populated large-scale networks. Considering adaptability, first step in the proposed system is efficient deployment of data gathering center as shown in Figure 3. In order to maintain an adaptable process, the proposed model starts with an effective deployment of data gathering center as shown in Figure 3. Sensing devices can either be deployed in a 2D or 3D space depending on application and available surface terrain.

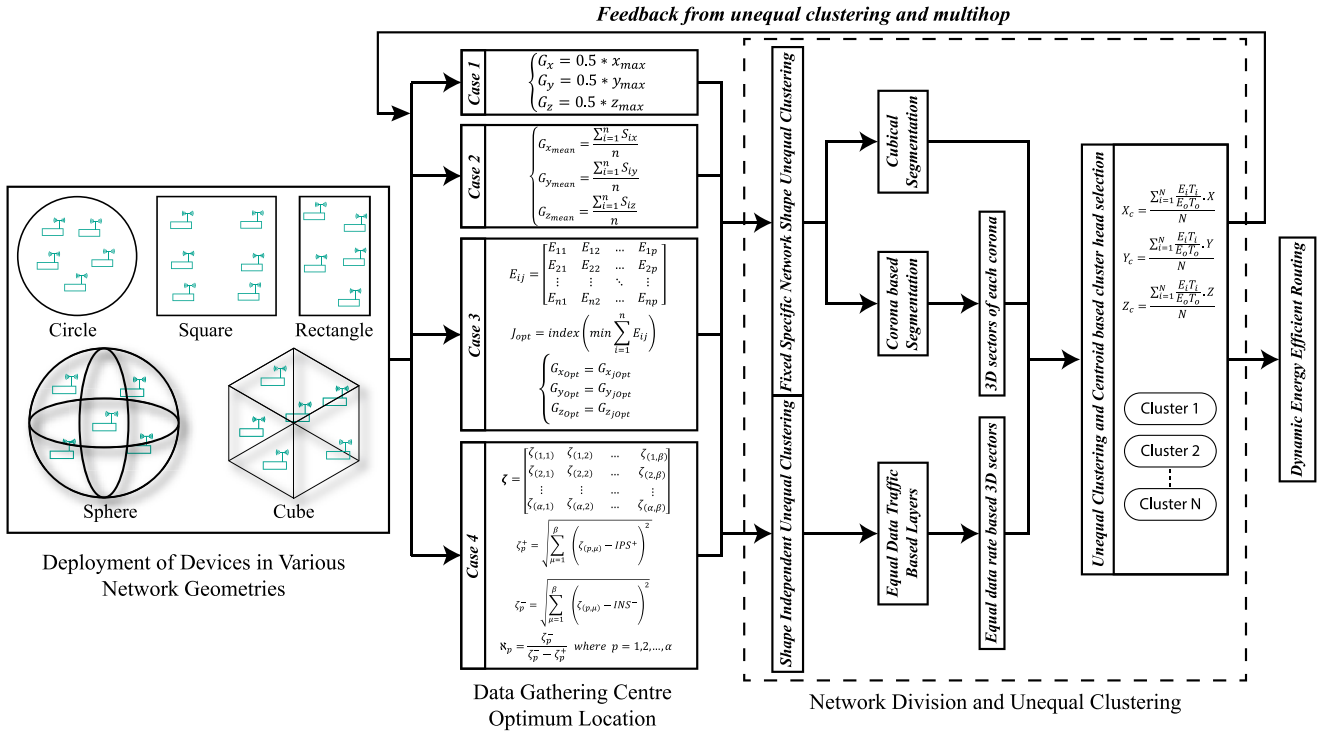

FIGURE 3. A system model proposed for adaptable flexible and scalable energy efficient hierarchical routing.

For this reason, adaptability of the proposed system is tested in prominent network geometries. Data gathering center is commonly located at the center of the network. Whereas energy efficiency and balanced load distribution can be achieved by determining an efficient location of data gathering center. Keeping energy efficiency as objective three other cases for the deployment of data gathering center in addition to commonly used centered deployment have been evaluated as shown in Figure 3.

A. CASE I

Traditionally, DGC is deployed at the center of the network. This case reflects a common deployment location of data gathering center. For a 3D network, the rectangular coordinates (G_x, G_y, G_z) of center of the network for DGC location can be mathematically determined by:

$$\begin{cases} G_x = 0.5 * x_{max} \\ G_y = 0.5 * y_{max} \\ G_z = 0.5 * z_{max} \end{cases} \tag{1}$$

where, $(x_{max} \times y_{max} \times z_{max})$ represents the 3D network volume. If the network is 2D the third coordinate in eq. 1 is not required and the network area reduces to $(x_{max} \times y_{max})$.

B. CASE II

In the second case an average of rectangular coordinates of devices in each dimension is calculated and DGC is deployed at the average coordinates as determined by:

$$\begin{cases} G_{x_{mean}} = \frac{\sum_{i=1}^{n} S_{ix}}{n} \\ G_{y_{mean}} = \frac{\sum_{i=1}^{n} S_{iy}}{n} \\ G_{z_{mean}} = \frac{\sum_{i=1}^{n} S_{iz}}{n} \end{cases} \tag{2}$$

where, $(G_{x_{mean}}, G_{y_{mean}}, G_{z_{mean}})$ are the rectangular coordinates of the fixed DGC for a 3D network and reduces to $(G_{x_{mean}}, G_{y_{mean}})$ for a 2D network.

C. CASE III

In a network of heterogeneous devices centrality may not be exactly at the mean of the coordinates. The device density in some regions may be different to the others. Similarly, devices in one region may be more energy rich than other regions. Therefore, to determine a common centrality point in terms of multiple parameters overall energy consumption is considered as ultimate objective.

In this 3rd case a region surrounding the point located at mean $(G_{x_{mean}}, G_{y_{mean}}, G_{z_{mean}})$ or $(G_{x_{mean}}, G_{y_{mean}})$ depending upon 3D or 2D network was considered. All the points located in this region are considered as alternatives for the deployment of data gathering center. The point offering minimum overall energy consumption is considered as optimal initial location of the data gathering center.

Let 'r' be the radius of the region containing all the points considered as alternatives for the location of data gathering

center. Then coordinates of alternatives can be determined as:

$$\begin{cases} G_{alt,X} = (G_{x_{mean}} - \Gamma) + \dfrac{X}{2} | X = 0, 1, 2, \ldots, 2\Gamma \\ G_{alt,Y} = (G_{y_{mean}} - \Gamma) + \dfrac{Y}{2} | Y = 0, 1, 2, \ldots, 2\Gamma \\ G_{alt,Z} = (G_{z_{mean}} - \Gamma) + \dfrac{Z}{2} | Z = 0, 1, 2, \ldots, 2\Gamma \end{cases} \quad (3)$$

The total number of alternative locations 'F' can be calculated as:

$$F = (2\Gamma + 1)^3 \quad (4)$$

The set of alternatives adjusts according to the network dimensions. Overall energy consumption of the network is computed for each alternative location. Let $E_{CON}1$ be the array containing information about energy consumption of each device from each alternative.

$$idx1 = arg\min_{ijk} ECON1[i, j, k] \quad (5)$$

$$\begin{cases} G_{x_{Opt}} = G_{alt,i} \\ G_{y_{Opt}} = G_{alt,j} \\ G_{z_{Opt}} = G_{alt,k} \end{cases} \quad (6)$$

The procedure for computation of optimal location of data gathering center is explained in algorithm 1.

The alternative from the set of candidate locations with minimum overall energy consumption is chosen as optimal location for the deployment of data gathering center. However, the bigger the network the complexity of this method increases with the increasing number of alternatives.

D. CASE IV

Due to the increasing computational complexity of energy efficient deployment as discussed in case iii, a multi criterion decision making technique TOPSIS [70] has been proposed. Distribution of heterogeneous attributes such as initial energy, data rate, and device density is considered to determine optimal location for the deployment of data gathering center. The set of alternative locations of data gathering center is computed using eq. 3.

Let 'E' be a set containing information on heterogeneous energies of the 'n' number of devices such that:

$$E = \{E_1, E_2, E_3, \ldots E_n\} \quad (7)$$

Energy of the m^{th} device can be calculated as:

$$E_m = E_o\,(1 + \beth) \quad (8)$$

where, E_o is the minimum initial energy of a device and '$\beth$' is a random number between 0 and 1. Similarly, T_m is the heterogeneous data traffic of each device calculated in a similar fashion as energy but in range $1000 - 4000$ packets.

An optimum location for the deployment of DGC has been considered as a multi-criterion problem based on distance, energy, device density, and available data traffic of each device. As the values of resources are measured in different scales, the min-max normalization technique has been used to obtain normalized values between a range [0 1] as follows:

$$\vartheta_o = \frac{\theta_o - \theta_{min}}{\theta_{max} - \theta_{min}} \quad (9)$$

where, ϑ_O is the normalized value of the parameter, "o", θ_o is the current value, θ_{max} and θ_{min} are the maximum and minimum values of a resource "o".

Algorithm 1 Location of Data Gathering Center Based on Minimum Energy Consumption

Require:
The number of devices n deployed within a network, their coordinates (x_i, y_i, z_i) ; $i = 1, 2, 3, \ldots, n$ of each sensor node, their heterogeneous initial energies denoted as S_i^E, their heterogeneous data rate denoted as S_i^T, radius 'r' from the point at mean of device coordinates in which alternative locations for the deployment of DGC are considered. Total number of clusters 'k'. Total number of alternative DGC locations as; $f = 1, 2, 3, \ldots, F$ and their coordinates in three-dimensional space using eq. 3.

Ensure: $G_{(.)}^{Opt} \leftarrow (G_{x_{Opt}}, G_{y_{Opt}}, G_{z_{Opt}})$

$S_i^E \leftarrow E_o\,(1 + \beth)$
$S_i^T \leftarrow T_o\,(1 + \tau)$
for $i \leftarrow 1$ to n do
  for $j \leftarrow 1$ to k do
    if $(i \leftarrow index(j))$
      $S_i^{type} =' CH'$
    else $S_i^{type} =' NN'$
    end if
    $D_{ij} \leftarrow \sqrt{\left(S_i^x - G_j^x\right)^2 + \left(S_i^y - G_j^y\right)^2 + \left(S_i^z - G_j^z\right)^2}$
  end for
  $S_i^{cluster} \leftarrow arg\min_{ij}(D_{ij})$
end for
for $i \leftarrow 1$ to n do
  for $j \leftarrow 1$ to k do
    if $(S_i^{type} = NN$ & $S_i^{cluster} = j)$
      $E_{CON_i} \leftarrow$ *Energy from* i^{th} *node to* j^{th} *CH*
    elseif $(S_i^{type} = CH)$
      $E_{CON_i} \leftarrow$ *Reception energy from all members*
    end if
  end for
end for
for $j \leftarrow 1$ to k do
  for $f \leftarrow 1$ to F do
    $D_{jf} \leftarrow \sqrt{\left(S_j^x - G_f^x\right)^2 + \left(S_j^y - G_f^y\right)^2 + \left(S_j^z - G_f^z\right)^2}$
    $E_{CON_{jf}} \leftarrow$ *Energy from* j^{th} *CH to* f^{th} *location*
  end for
  $E_f = \sum_{j=1}^{k}(E_{CON_{jf}})$
end for
$Opt = arg\min_f(E_f)$
$\left(G_{Opt}^x, G_{Opt}^x, G_{Opt}^x\right) \leftarrow \left(G_{Opt}^x, G_{Opt}^x, G_{Opt}^x\right)$

It is assumed that the suitable location for the DGC is within the central segment of the network such that its coordinates can be ranging from (0, 0, 0) to (Γ, Γ, Γ). To compute the impact of each parameter within this range let '$\boldsymbol{\zeta}$' be a matrix containing normalized values of all resources and its impact in energy calculation for each alternative location of DGC.

$$\boldsymbol{\zeta} = \begin{bmatrix} \zeta_{(1,1)} & \zeta_{(1,2)} & \zeta_{(1,3)} & \cdots & \zeta_{(1,\beta)} \\ \zeta_{(2,1)} & \zeta_{(2,2)} & \zeta_{(2,3)} & \cdots & \zeta_{(2,\beta)} \\ \zeta_{(3,1)} & \zeta_{(3,2)} & \zeta_{(3,3)} & \cdots & \zeta_{(3,\beta)} \\ \vdots & \vdots & \vdots & \cdots & \vdots \\ \zeta_{(\alpha,1)} & \zeta_{(\alpha,2)} & \zeta_{(\alpha,3)} & \cdots & \zeta_{(\alpha,\beta)} \end{bmatrix} \tag{10}$$

where, $\zeta_{\alpha,\beta}$ is the value of βth parameter of each device calculated from αth alternative location of the DGC.

Parameters where high value is desired such as initial energy and density of the devices are declared as ideal positive solution IPS^+ and is computed as:

$$IPS^+ = \max\left\{\left(\zeta_{(1,\mu)}\right), \left(\zeta_{(2,\mu)}\right), \ldots, \left(\zeta_{(\alpha,\mu)}\right)\right\}, \forall\mu \in \beta \tag{11}$$

Parameters where low value is desired such as data traffic, and distance of devices are declared as ideal negative solution INS^- and is computed as:

$$INS^- = \min\left\{\left(\zeta_{(1,\mu)}\right), \left(\zeta_{(2,\mu)}\right), \ldots, \left(\zeta_{(\alpha,\mu)}\right)\right\}, \forall\mu \in \beta \tag{12}$$

For each parameter, the difference of the values from IPS^+ and INS^- for each candidate location of DGC are calculated as follows:

$$\zeta_p^+ = \sqrt{\sum_{\mu=1}^{\beta}(\zeta_{(p,\mu)} - IPS^+)^2} \; where\; p = 1, 2, 3 \ldots \alpha \tag{13}$$

$$\zeta_p^- = \sqrt{\sum_{\mu=1}^{\beta}(\zeta_{(p,\mu)} - INS^-)^2} \; where\; p = 1, 2, 3 \ldots \alpha \tag{14}$$

where, ζ_p^+ and ζ_p^- represent the difference of potential location of DGC from IPS^+ and INS^- respectively. Rank of each potential location for the deployment of DGC in the central segment is then calculated as:

$$\aleph_p = \frac{\zeta_p^-}{\zeta_p^- - \zeta_p^+} \; where\; p = 1, 2, 3 \ldots \alpha \tag{15}$$

Location with the best rank can be chosen as optimum deployment location for the data gathering center.

The alternative location with best value of rank $\aleph_p$ is chosen as optimal location for the deployment of data gathering center. Due to constraints in some locations as a result of varying terrains if data gathering center cannot be deployed at the alternative with best rank the alternative with second best value is chosen as the next optimum location.

Algorithm 2 Optimal Location for the Deployment of Data Gathering Center Using a Multi-Criterion Decision Making Technique TOPSIS

Require:
The number of devices n deployed within the 3D network, the coordinates (x_i, y_i, z_i) ; $i = 1, 2, 3, \ldots, n$ of each sensor node, their heterogeneous energies denoted as S_i^E, their heterogeneous data traffic denoted as S_i^T, radius 'r' from the point at mean of device coordinates in which alternative locations for the deployment of DGC are considered. Total number of clusters 'k'. Total number of alternative DGC locations as; $f = 1, 2, 3, \ldots, F$ and their coordinates in three-dimensional space using eq. 3.

Ensure: $G_{(.)}^{TOPSIS} \leftarrow \alpha with \max\{\aleph_p\}$

$S_i^E \leftarrow E_o\,(1 + \beth)$
$S_i^T \leftarrow T_o\,(1 + \tau)$
for $j \leftarrow 1$ to k do
  for $f \leftarrow 1$ to F do
    $D_{jf} \leftarrow \sqrt{\left(S_j^x - G_f^x\right)^2 + \left(S_j^y - G_f^y\right)^2 + \left(S_j^z - G_f^z\right)^2}$
  end for
end for
$min\theta_{En} \leftarrow \min S_i^E$
$max\theta_{En} \leftarrow \max S_i^E$
$min\theta_{Tr} \leftarrow \min S_i^T$
$max\theta_{Tr} \leftarrow \max S_i^T$
$min\theta_{Dist} \leftarrow \min D_{jf}$
$max\theta_{Dist} \leftarrow \max D_{jf}$
Normalize S_i^E
Normalize S_i^T
Normalize D_i^K
for $i \leftarrow 1$ to α do
  for $j \leftarrow 1$ to β do
    $\boldsymbol{\zeta} \leftarrow \zeta_{\alpha,\beta}$
    $IPS^+ \leftarrow \max\left\{\zeta_{(\alpha,\mu)}\right\}, \;\forall\; \mu\in\beta$
    $INS^- \leftarrow \max\left\{\zeta_{(\alpha,\mu)}\right\}, \;\forall\; \mu\in\beta$
    $\zeta_p^+ = \sqrt{\sum_{\mu=1}^{\beta}(\zeta_{(p,\mu)} - IPS^+)^2} wherep = 1, 2, 3 \ldots \alpha$
    $\zeta_p^- = \sqrt{\sum_{\mu=1}^{\beta}(\zeta_{(p,\mu)} - INS^-)^2} wherep = 1, 2, 3 \ldots \alpha$
    $\aleph_p = \frac{\zeta_p^-}{\zeta_p^- - \zeta_p^+} \; where\; p = 1, 2, 3 \ldots \alpha$
  end for
end for
return $\aleph_p$

IV. PROPOSED NETWORK SEGMENTATION

In this section network segmentation has been discussed. For an adaptive scheme considering deployment of heterogeneous devices in 2D or 3D space, the network can take any shape. A range of popular network shapes in both 2D and 3D spaces have been shown in Figure 4.

In this work we consider two prominent segmentations in cubical and spherical 3D networks. For a spherical shape network, a 3D corona and sectors-based segmentation is developed and for a cubical shape network a cubical virtual subdivision of network is developed. These segmentation schemes help in obtaining the information about distribution of device parameters in smaller regions using divide-and-rule

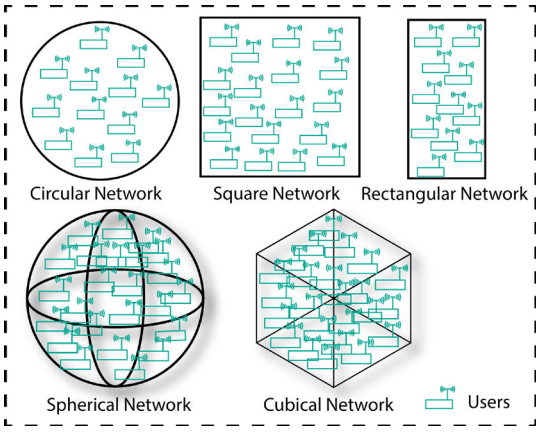

FIGURE 4. Common network shapes in 2D and 3D environments.

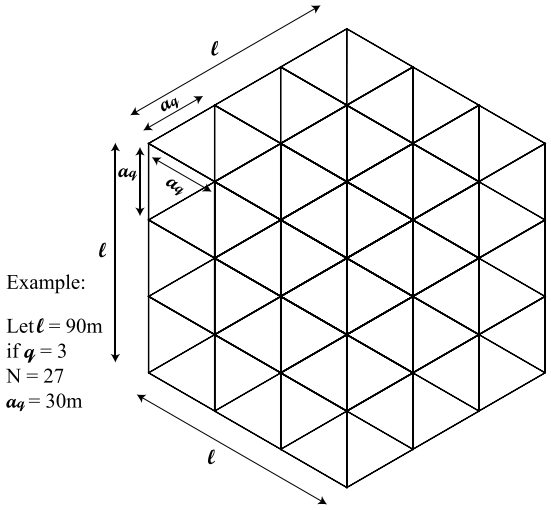

FIGURE 5. 3D cubical network segmented into sub-cubes.

approach. In the next sub sections a discussion on the two segmentation schemes has been made:

A. CUBICAL SEGMENTATION

In this segmentation the whole network is divided into 'N' non-overlapping uniform virtual sub-cubes of dimensions $(a \times a \times a)$ each as shown in Figure 5.

Where, $q = \sqrt[3]{N}$ is the number of divisions in each dimension so that,

$$a = \frac{l}{q} \tag{16}$$

where, 'l' is the length of each side of the cube.

Let 'Q' be the set of all the virtual sub-cubes within the network which is defined as:

$$\boldsymbol{Q} = \left\{Q_{hjk} | h, j, k = 1, 2, \ldots, q\right\} \tag{17}$$

Therefore, for a given virtual sub-cube Q_{hjk} the boundary coordinates $\left(a_{h-1} \times a_{j-1} \times a_{k-1}\right)$ and $\left(a_h \times a_j \times a_k\right)$ of the virtual sub cube can be computed as:

$$a_{h-1} = \frac{h-1}{q} * l \text{ and } a_h = \frac{h}{q} * l \tag{18.1}$$

$$a_{j-1} = \frac{j-1}{q} * l \text{ and } a_j = \frac{j}{q} * l \tag{18.2}$$

$$c_{k-1} = \frac{k-1}{q} * l \text{ and} \tag{18.3}$$

So that $\boldsymbol{Q}$ is a 3D matrix of dimensions $(h \times j \times k)$. For a sensing node '$S_{(m)}$' such that m is a real number and $1 \leq m \leq n$.

$$\{\boldsymbol{S}_m \in Q_{hjk} | a_{h-1} \leq S_{hx} \leq a_h \text{ and } a_{j-1} \leq S_{jy} \leq a_j \text{ and } a_{k-1} \leq S_{kz} \leq a_k \tag{19}$$

Let $\boldsymbol{N}_{hjk}$ be 3D matrix containing information about number of nodes in each virtual sub cube such that:

$$N_{hj1} = \begin{bmatrix} N_{111} & \cdots & N_{1j1} \\ \vdots & \ddots & \vdots \\ N_{h11} & \cdots & N_{ij1} \end{bmatrix} \text{ for } h, j = 1, 2, \ldots, q$$

$$N_{hj2} = \begin{bmatrix} N_{112} & \cdots & N_{1j2} \\ \vdots & \ddots & \vdots \\ N_{h12} & \cdots & N_{hj2} \end{bmatrix} \text{ for } h, j = 1, 2, \ldots, q$$

$$\vdots$$

$$k = 1, 2, \ldots, q$$

$$N_{hjk} = \begin{bmatrix} N_{11k} & \cdots & N_{1jk} \\ \vdots & \ddots & \vdots \\ N_{h1k} & \cdots & N_{1jk} \end{bmatrix} \text{ for } h, j = 1, 2, \ldots, q \tag{20}$$

Segmentation provides the advantage of obtaining local information about several regions of the network such as density, data traffic and energies.

Let '$\boldsymbol{T}$' be 3D array containing information about data rate in each virtual sub-cube of the network such that:

$$T_{hj1} = \begin{bmatrix} T_{111} & \cdots & T_{1j1} \\ \vdots & \ddots & \vdots \\ T_{h11} & \cdots & T_{hj1} \end{bmatrix} \text{ for } h, j = 1, 2, \ldots, q$$

$$T_{hj2} = \begin{bmatrix} T_{112} & \cdots & T_{1j2} \\ \vdots & \ddots & \vdots \\ T_{h12} & \cdots & T_{hj2} \end{bmatrix} \text{ for } h, j = 1, 2, \ldots, q$$

$$\vdots$$

$$k = 1, 2, \ldots, q$$

$$T_{hjk} = \begin{bmatrix} T_{11k} & \cdots & T_{1jk} \\ \vdots & \ddots & \vdots \\ T_{h1k} & \cdots & T_{1jk} \end{bmatrix} \; for\; h, j = 1, 2, \ldots, q \qquad (21)$$

Similarly, $\boldsymbol{E}$ is a $(h \times j \times k)$ array with information on residual energies of devices within the corresponding virtual sub-cube.

Once the virtual sub-cubes-based segmentation is configured and information on nodes in each virtual sub-cube is obtained, a centroid on the basis of distribution function in each sub-cube is calculated. The choice of cluster head is made according to the distance from the centroid. Based on the distance of a virtual sub-cube from the data gathering center the number of cluster heads is calculated using geometric progression such that $NCH_1 = 1$; $NCH_2 = 2\,(NCH_1)$; $NCH_3 = 4\,(NCH_1)$ and $NCH_{\mathrm{N}} = 2^{\mathrm{N}-1}\,(NCH_1)$. Where, NCH is the number of cluster heads in each sub-cube and N is the level of the virtual sub-cube based on the distance from the inner most sub-cube. A distribution centroid based on the parameters of devices in a sub-cube is calculated using:

$$\begin{aligned} X_c &= \frac{\sum_{i=1}^{N} \frac{E_i T_i}{E_o T_o}.X_i}{N} \\ Y_c &= \frac{\sum_{i=1}^{N} \frac{E_i T_i}{E_o T_o}.Y_i}{N} \\ Z_c &= \frac{\sum_{i=1}^{N} \frac{E_i T_i}{E_o T_o}.Z_i}{N} \end{aligned} \qquad (22)$$

According to number of cluster heads 'NCH_{N}' in each sub-cube, devices with maximum energy closest to the centroid are selected as cluster heads. Coordinates of centroid in each sub-cube are calculated using eq. (22) where, N is the total number of devices in each sub-cube and E_i and T_i are the residual energies and data rate of i^{th} device in the sub-cube.

Algorithm 3 Cubical Network Segmentation Scheme and Cluster Head Selection Based on Centroid of Distribution of Devices Parameters in Each Segment

Require:
The number of devices n deployed within the 3D network, their coordinates (x_i, y_i, z_i) ; $i = 1, 2, 3, \ldots, n$ of each sensor node, their heterogeneous energies denoted as S_i^E, their heterogeneous data traffic denoted as S_i^T. Total number of sub-cubes 'N' and length 'l' of each side of 3D network.

Ensure:
$S_{(.)}^{ch-subcube} \leftarrow devices with \min\left\{D_{C_{hjk}}^{i}\right\}\ \&\ \max\left\{E_{hjk}\right\}$

$l \leftarrow$ length of each side of the network
$N \leftarrow Total\ number\ of\ sub-cubes$
$q \leftarrow \sqrt[3]{N}$
for $i \leftarrow 1$ to n do
  $S_i^E \leftarrow E_o\,(1 + \beth)$
  $S_i^T \leftarrow T_o\,(1 + \tau)$
  for $h \leftarrow 1$ to q
    for $j \leftarrow 1$ to q
      for $k \leftarrow 1$ to q
        $a_{h-1} \leftarrow \frac{h-1}{q} * l$
        $a_h \leftarrow \frac{h}{q} * l$
        $a_{j-1} \leftarrow \frac{j-1}{q} * l$
        $a_j \leftarrow \frac{j}{q} * l$
        $c_{k-1} \leftarrow \frac{k-1}{q} * l$
        $c_k \leftarrow \frac{k}{q} * l$
        if $(a_{h-1} \leq S_i^x \leq a_h)$
          if $(a_{j-1} \leq S_i^y \leq a_j)$
            if $\left(a_{k-1} \leq S_i^y \leq a_k\right)$
              $N_{hjk} \leftarrow N_{hjk} + 1$
              $T_{hjk} \leftarrow T_{hjk} + T_i$
              $E_{hjk} \leftarrow E_{hjk} + E_i$
              $X_{C_{hjk}} \leftarrow \frac{\sum_{i=1}^{N_{hjk}} \frac{E_i T_i}{E_o T_o}.X_i}{N_{hjk}}$
              $Y_{C_{hjk}} \leftarrow \frac{\sum_{i=1}^{N_{hjk}} \frac{E_i T_i}{E_o T_o}.Y_i}{N_{hjk}}$
              $Z_{C_{hjk}} \leftarrow \frac{\sum_{i=1}^{N_{hjk}} \frac{E_i T_i}{E_o T_o}.Z_i}{N_{hjk}}$
              $D_{C_{hjk}}^{i} \leftarrow Distance\ of\ node\ in\ each\ cube\ to\ the\ centroid$
              end if
            end if
          end if
        end for
      end for
    end for
  end for
  for $h \leftarrow 1$ to q
    for $j \leftarrow 1$ to q
      for $k \leftarrow 1$ to q
        $D_{C_{min}} \leftarrow \min\left\{D_{C_{hjk}}^{i}\right\}$
        $E_{max} \leftarrow \max\left\{E_{hjk}\right\}$
        for $i \leftarrow 1$ to n
          if $\left(D_{C_{min}} \leftarrow D_{C_{hjk}}^{i}\ \&\&\ E_{max} \leftarrow E_i\right)$
            $S_i^{type} \leftarrow CH$
          end if
        end for
      end for
    end for
  end for
  Return $S_{(.)}^{type}$

The proposed segmentation determines the resources and calculates a centroid of distribution in each sub cube. Devices with minimum distance and maximum residual energy are chosen as cluster head of the cub cube region. The number of cluster heads in a sub-cube is computed based on the distance of the sub-cube from DGC.

B. SPHERICAL SEGMENTATION

For a spherical shape network, the network is divided into 'q' non-overlapping concentric spherical coronas of equal volume as shown in Figure 6, such that the radius of each sphere from origin can be calculated as:

$$rq = \sqrt[3]{\frac{3q}{4\pi}} \qquad (23)$$

The range of each corona segment can be determined as:

$$\Re q = rq - rq_{-1} \qquad (24)$$

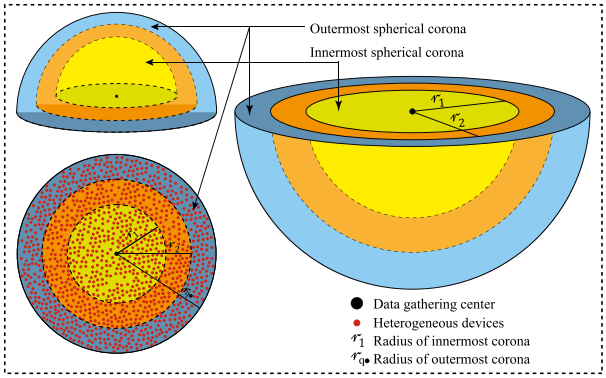

FIGURE 6. Spherical network segmentation.

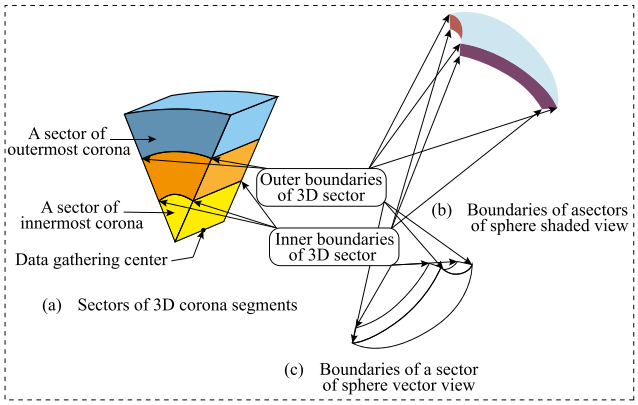

FIGURE 7. Sectors of 3D coronas and their boundaries.

The volume of each corona segment can be calculated as:

$$V_{\mathfrak{q}} = \frac{4}{3}\pi\left[r^3_{\mathfrak{q}} - r^3_{\mathfrak{q}-1}\right] \tag{25}$$

'$\Re_1$' is the radius of the inner most spherical corona using eq. (24) such that $\Re_1 \leq Trans_{min}$, and $Trans_{min}$ is the minimum transmission range. Let r_m be the radius of m^{th} corona then equal volume condition for each concentric corona implies that:

$$\frac{4}{3}\pi\left(r_m\right)^3 - \frac{4}{3}\pi\left(r_{m-1}\right)^3 = \frac{4}{3}\pi\left(r_{m-1}\right)^3$$

Thus r_m can be computed as:

$$\begin{aligned}\left(r_m\right)^3 &= \left(r_{m-1}\right)^3 + \left(r_{m-1}\right)^3\\ r_m &= \sqrt[3]{2} * r_{m-1}\end{aligned} \tag{26}$$

Therefore, based on the maximum radius r_{max}, which is the boundary of the spherical network DGC calculates the volumes and boundaries of each spherical corona using eq. (26) until it reaches $Trans_{min}$ which is the radius of first spherical corona.

The next step is division of each corona segment into 3D sectors as shown in Figure 7 and creating unequal clusters within each segment. Sectors formation starts from the center of the spherical network and corners of each sector can be worked using eq. IV-B:

Let $\left(G_x, G_y, G_z\right)$ be the center of the sphere.

$$\mathrm{x}_{\mathfrak{f}\mathfrak{g}\mathfrak{h}} = r_{\mathfrak{f}}\cos\left(\varphi_{\mathfrak{g}}\right)\cos\left(\vartheta_{\mathfrak{h}}\right) \tag{27.1}$$

$$\mathcal{Y}_{\mathfrak{f}\mathfrak{g}\mathfrak{h}} = r_{\mathfrak{f}}\cos\left(\varphi_{\mathfrak{g}}\right)\sin\left(\vartheta_{\mathfrak{h}}\right) \tag{27.2}$$

$$\mathrm{z}_{\mathfrak{f}\mathfrak{g}\mathfrak{h}} = r_{\mathfrak{f}}\sin\left(\varphi_{\mathfrak{g}}\right) \tag{27.3}$$

where $r_{\mathfrak{f}}$, $\varphi_{\mathfrak{g}}$ and $\varphi_{\mathfrak{h}}$ can be determined as:

$$r_{\mathfrak{f}} = r_1, r_2, \ldots, r_{max} \tag{28.1}$$

$$\varphi_{\mathfrak{g}} = \{0, \frac{\pi}{4}, \frac{\pi}{2}, \frac{3\pi}{4}, \pi, \frac{5\pi}{4}, \frac{3\pi}{2}, \frac{7\pi}{4}, 2\pi\} \tag{28.2}$$

$$\varphi_{\mathfrak{h}} = \{0, \frac{\pi}{4}, \frac{\pi}{2}, \frac{3\pi}{4}, \pi, \frac{5\pi}{4}, \frac{3\pi}{2}, \frac{7\pi}{4}, 2\pi\} \tag{28.3}$$

Centroid of each sector is calculated and the nearest device to centroid point with maximum energy is selected as cluster head.

Algorithm 4 Spherical Corona-Based Segmentation and 3D Sectoring for Unequal Clustering and Centroid Based Choice of Cluster Heads in Each Sector

Require:

The number of devices 'n' deployed within the 3D spherical network, their coordinates (x_i, y_i, z_i) ; $i = 1, 2, 3, \ldots, n$ of each sensor node, their heterogeneous energies denoted as S_i^E, their heterogeneous data traffic denoted as S_i^T. Radius r_{max} of spherical shape 3D network.

Ensure: $S^{ch-sphere}_{(.)} \leftarrow devices\ with\ \min\left\{D^i_{\mathfrak{c}_{\mathfrak{f}\mathfrak{g}\mathfrak{h}}}\right\}$ and $\max\{\mathrm{E}_i\}$

$r_{max} \leftarrow$ maximum radius of network
$r_m \leftarrow$ Radius of m^{th} spherical corona segment (It will start from $r_m \leftarrow r_{max}$)
if $(r_m < Trans_{min})$ do
  $r_m \leftarrow \sqrt[3]{2} * r_{m-1}$
  $m \leftarrow m + 1$
end if
for $i \leftarrow 1$ to n do
  $S_i^E \leftarrow E_o\left(1 + \beth\right)$
  $S_i^T \leftarrow T_o\left(1 + \tau\right)$
end for
$\vartheta_o \leftarrow 0$
$\varphi_o \leftarrow -\frac{\pi}{2}$
for $\mathfrak{f} \leftarrow 1$ to m
  for $\mathfrak{g} \leftarrow 1$ to 9
    for $\mathfrak{h} \leftarrow 1$ to 9
      $r_{\mathfrak{f}} \leftarrow r_m$
      $\varphi_{\mathfrak{g}} \leftarrow \varphi_{\mathfrak{g}} + \frac{\pi}{4}$
      $\vartheta_{\mathfrak{h}} \leftarrow \vartheta_{\mathfrak{h}} + \frac{\pi}{4}$
      $\mathrm{x}_{\mathfrak{f}\mathfrak{g}\mathfrak{h}} \leftarrow r_{\mathfrak{f}}\cos\left(\varphi_{\mathfrak{g}}\right)\cos\left(\vartheta_{\mathfrak{h}}\right)$
      $\mathcal{Y}_{\mathfrak{f}\mathfrak{g}\mathfrak{h}} \leftarrow r_{\mathfrak{f}}\cos\left(\varphi_{\mathfrak{g}}\right)\sin\left(\vartheta_{\mathfrak{h}}\right)$
      $\mathrm{z}_{\mathfrak{f}\mathfrak{g}\mathfrak{h}} \leftarrow r_{\mathfrak{f}}\sin\left(\varphi_{\mathfrak{g}}\right)$
    end for
  end for
end for
for $i \leftarrow 1$ to n do
  for $\mathfrak{f} \leftarrow 1$ to m
    for $\mathfrak{g} \leftarrow 1$ to 9
      for $\mathfrak{h} \leftarrow 1$ to 9
        if $(\mathrm{x}_{\mathfrak{f}-1,\mathfrak{g}-1,\mathfrak{h}-1} \leq S_i^x \leq \mathrm{x}_{\mathfrak{f}\mathfrak{g}\mathfrak{h}})$
          if $(\mathcal{Y}_{\mathfrak{f}-1,\mathfrak{g}-1,\mathfrak{h}-1} \leq S_i^y \leq \mathcal{Y}_{\mathfrak{f}\mathfrak{g}\mathfrak{h}})$
            if $(\mathrm{z}_{\mathfrak{f}-1,\mathfrak{g}-1,\mathfrak{h}-1} \leq S_i^z \leq \mathrm{z}_{\mathfrak{f}\mathfrak{g}\mathfrak{h}})$
              $\mathrm{N}_{\mathfrak{f}\mathfrak{g}\mathfrak{h}} \leftarrow \mathrm{N}_{\mathfrak{f}\mathfrak{g}\mathfrak{h}} + 1$
              $\mathrm{T}_{\mathfrak{f}\mathfrak{g}\mathfrak{h}} \leftarrow \mathrm{T}_{\mathfrak{f}\mathfrak{g}\mathfrak{h}} + 1$
              $\mathrm{E}_{\mathfrak{f}\mathfrak{g}\mathfrak{h}} \leftarrow \mathrm{E}_{\mathfrak{f}\mathfrak{g}\mathfrak{h}} + 1$

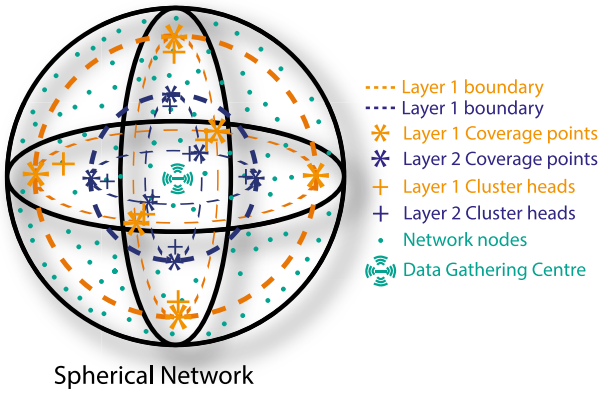

FIGURE 8. Equal data traffic-based segmentation and unequal cluster formation for balanced energy hierarchical routing.

$$x_{c-fgh} \leftarrow \frac{\sum_{i=1}^{N_{fgh}} \frac{E_i T_i}{E_o T_o} . x}{N_{fgh}}$$

$$y_{c-fgh} \leftarrow \frac{\sum_{i=1}^{N_{fgh}} \frac{E_i T_i}{E_o T_o} . y}{N_{fgh}}$$

$$z_{c-fgh} \leftarrow \frac{\sum_{i=1}^{N_{fgh}} \frac{E_i T_i}{E_o T_o} . z}{N_{fgh}}$$

$D^i_{c_{fgh}} \leftarrow$ *Distance of nodes in each sector to centroid*

end if
end if
end if
end for
end for
end for
end for
for $i \leftarrow 1$ to n do
  for $f \leftarrow 1$ to m
    for $g \leftarrow 1$ to 9
      for $h \leftarrow 1$ to 9
        $Distmin \leftarrow \min\left\{D^i_{c_{fgh}}\right\}$
        $E_r max \leftarrow \max\left\{E_{fgh}\right\}$
        if $\left(Distmin \leftarrow D^i_{c_{fgh}} \;\&\&\; E_r max \leftarrow E_i\right)$
          $S_i^{type} \leftarrow CH$
        end if
      end for
    end for
  end for
end for
Return $S^{type}_{(.)}$

The proposed segmentation determines the resources and calculates a centroid of distribution in each 3D sector. Devices with minimum distance and maximum residual energy are chosen as cluster head of the 3D sector. The number of cluster heads in a sub-cube is computed based on the distance of the sub-cube from DGC.

V. ADAPTIVE UNEQUAL CLUSTERUNG TECHNIQUE

Although proposed unequal clustering techniques based on shape specific segmentation produce good results in terms of increased network lifetime and balanced energy operation but are not adaptable to networks with varying shapes. Therefore, a shape independent unequal clustering algorithm is proposed in this section. Network is divided into layers of equal transmission rate instead of shape-based segments.

Let 'D_i' be the distance of i^{th} device from data gathering center (G_x, G_y, G_z). All the devices have heterogeneous initial energies and data traffic rates in a given range. Data gathering center obtains information about locations, initial energies, and data rates of all devices. The devices are grouped into layers of equal data rate based on their distance from data gathering center. Figure 8 shows the layer boundaries of a 3-layer network structure. If T_{L1} is the data traffic in the outermost layer. The adaptive unequal clustering algorithm continues to add traffic rate and add devices in first layer starting from the farthest device until the condition $T_{L1} \geq \frac{\sum T}{4}$ is reached. The distance of last device from the data gathering center is considered as the radial boundary of the layer 1. The algorithm continues to divide devices in concentric 3D layers until the first device at $Trans_{min}$ distance from data gathering center is reached.

Each layer is then divided into eight sectors of equal data rate. A centroid of distribution is determined in each sector and the devices with abundant resources closer to the centroid are chosen as cluster heads. The total number of cluster heads in each sector is computed based on its layer number. The operation of shape independent adaptive unequal clustering has been presented in algorithm 5.

Algorithm 5 Adaptive Unequal Clustering for Shape Independent 3D Network of Heterogeneous Devices

Require:
The number of devices n deployed within any shape network, their coordinates (x_i, y_i, z_i) ; $i = 1, 2, 3, \ldots, n$ of each sensor node, their heterogeneous energies denoted as S_i^E, their heterogeneous data traffic denoted as S_i^T. The total number of layers of data traffic η.

Ensure: $S^{ch-dynamic}_{(.)} \leftarrow$ *devices with* $\min\left\{D^i_{c_{Fgh}}\right\}$ & $\max^{E_i}_{(.)}$

for $i \leftarrow 1$ to n do
  $S_i^E \leftarrow E_o\,(1 + \beth)$
  $S_i^T \leftarrow T_o\,(1 + \tau)$
  $D_i \leftarrow \sqrt{\left(S_i^x - G_x\right)^2 + \left(S_i^y - G_y\right)^2 + \left(S_i^z - G_z\right)^2}$
end for
$I \leftarrow index(sort\{D\})$
$T \leftarrow T(I)$
$D_{L0} \leftarrow \max\{D\}$
for $i \leftarrow 1$ to n do
  if $(T_{L1} \leq \frac{\sum T}{4})$ do
    $T_{L1} \leftarrow T_{L1} + T(i)$
  elseif $(\frac{\sum T}{4} \leq T_{L1} \leq \sum T)$
    if $(T_{L2} \leq \frac{\sum T}{4})$ do
      $T_{L2} \leftarrow T_{L2} + T(i)$
    elseif $(\frac{\sum T}{2} \leq T_{L2} \leq \frac{3\sum T}{4})$ do
      if $(T_{L3} \leq \frac{\sum T}{4})$ do
        $T_{L3} \leftarrow T_{L3} + T(i)$
      else do
        $T_{L4} \leftarrow T_{L4} + T(i)$
      end if

```
    end if
  end if
end for
θ_o = 0
Φ_o = −π/2
for i ← 1 to n do
  for F ← 1 to 5
    for g ← 1 to 9
      for h ← 1 to 9
        T_{F−1,g,h} ← D_{L(F−1)}
        T_{F,g,h} ← D_{L,F}
        if (T_{sec−g} ≤ (Σ T_{L,g}) / 8) do
          T_{sec−g} = T_{sec−g} + T(i)
          Φ_g = Φ_g + +
          θ_h = θ_h + +
          x_{F,g,h} = T_F cos(Φ_g) cos(θ_h)
          y_{F,g,h} = T_F cos(Φ_g) sin(θ_h)
          z_{F,g,h} = T_F sin(Φ_g)
        end if
      end for
    end for
  end for
end for
for i ← 1 to n do
  for F ← 1 to 5
    for g ← 1 to 9
      for h ← 1 to 9
        if (x_{F−1,g−1,h−1} ≤ S_i^x ≤ x_{F,g,h})
          if (y_{F−1,g−1,h−1} ≤ S_i^y ≤ y_{F,g,h})
            if (z_{F−1,g−1,h−1} ≤ S_i^z ≤ z_{F,g,h})
              N_{F,g,h} ← N_{F,g,h} + 1
              T_{F,g,h} ← T_{F,g,h} + T(i)
              E_{F,g,h} ← E_{F,g,h} + E(i)
              x_{c,F,g,h} ← (Σ_{i=1}^{N_{F,g,h}} (E_i T_i)/(E_o T_o) . x) / N_{f,F,g,h}
              y_{c,F,g,h} ← (Σ_{i=1}^{N_{F,g,h}} (E_i T_i)/(E_o T_o) . y) / N_{f,F,g,h}
              z_{c,F,g,h} ← (Σ_{i=1}^{N_{F,g,h}} (E_i T_i)/(E_o T_o) . z) / N_{f,F,g,h}
              D^i_{c,F,g,h} ← Distance of nodes in each sector to centroid
            end if
          end if
        end if
      end for
    end for
  end for
end for
for i ← 1 to n do
  for F ← 1 to 5
    for g ← 1 to 9
      for h ← 1 to 9
        Distmin ← min{D^i_{c,F,g,h}}
        E_max ← max{E_{F,g,h}}
        if (Distmin ← D^i_{c,F,g,h} && E_max ← E_i)
          S_i^type ← CH
        end if
      end for
    end for
  end for
end for
Return_(S^type)
```

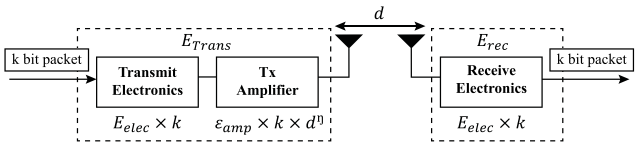

FIGURE 9. First order radio model.

TABLE 1. Simulation parameters.

Parameter	Value
Number of nodes	100
Initial energy of nodes	0.5 *to* 2*J*
Packet size (k)	$1000 - 4000\ bits$
Electronic circuitry (E_{elec})	$50\ nJ/bit/m^2$
Amplifier energy for free space (ε_{fs})	$10pJ/bit/m^2$
Amplifier energy for multipath (ε_{mp})	$0.0013\ pJ/bit/m^4$
Energy for data aggregation (E_{da})	$5\ nJ/bit$

VI. ENERGY MODEL

First order radio model is used to evaluate the proposed techniques [57]. This radio model uses E_{elec} as energy used by transmitter or receiver electronics in the transceiver circuit as shown in Figure 9. Both channel models i.e., free space with d^2 power loss, and multi-path fading with d^4 power loss are used by the transmitter amplifier. The radio of each device is equipped with power control capabilities and can adjust to minimum energy spent to reach the required recipient. Thus, to transmit k-bit message at a distance 'd' using this model the radio of each device expends:

$$E_{Trans}(k,d) = \begin{cases} k \times E_{elec} + k \times \varepsilon_{fs} \times d^2; \ d < d_o \\ k \times E_{elec} + k \times \varepsilon_{mp} \times d^4; \ d \geq d_o \end{cases} \quad (29.1)$$

Similarly, to receive this message, the device radio expends:

$$E_{rec}(k) = k \times E_{elec} \quad (29.2)$$

Here, E_{elec} is the unit energy dissipation for transmitter electronics or receiver electronics. ε_{fs} is the amplifier energy in the free space model, while ε_{mp} is the amplifier energy in the multi-path model, and $d_o$is the threshold defined as:

$$d_o = \sqrt{\varepsilon_{fs}/\varepsilon_{mp}} \quad (29.3)$$

VII. RESULTS AND DISCUSSIONS

In this section, the performance of proposed techniques has been evaluated using MATLAB simulations. The proposed techniques have been evaluated in various phases

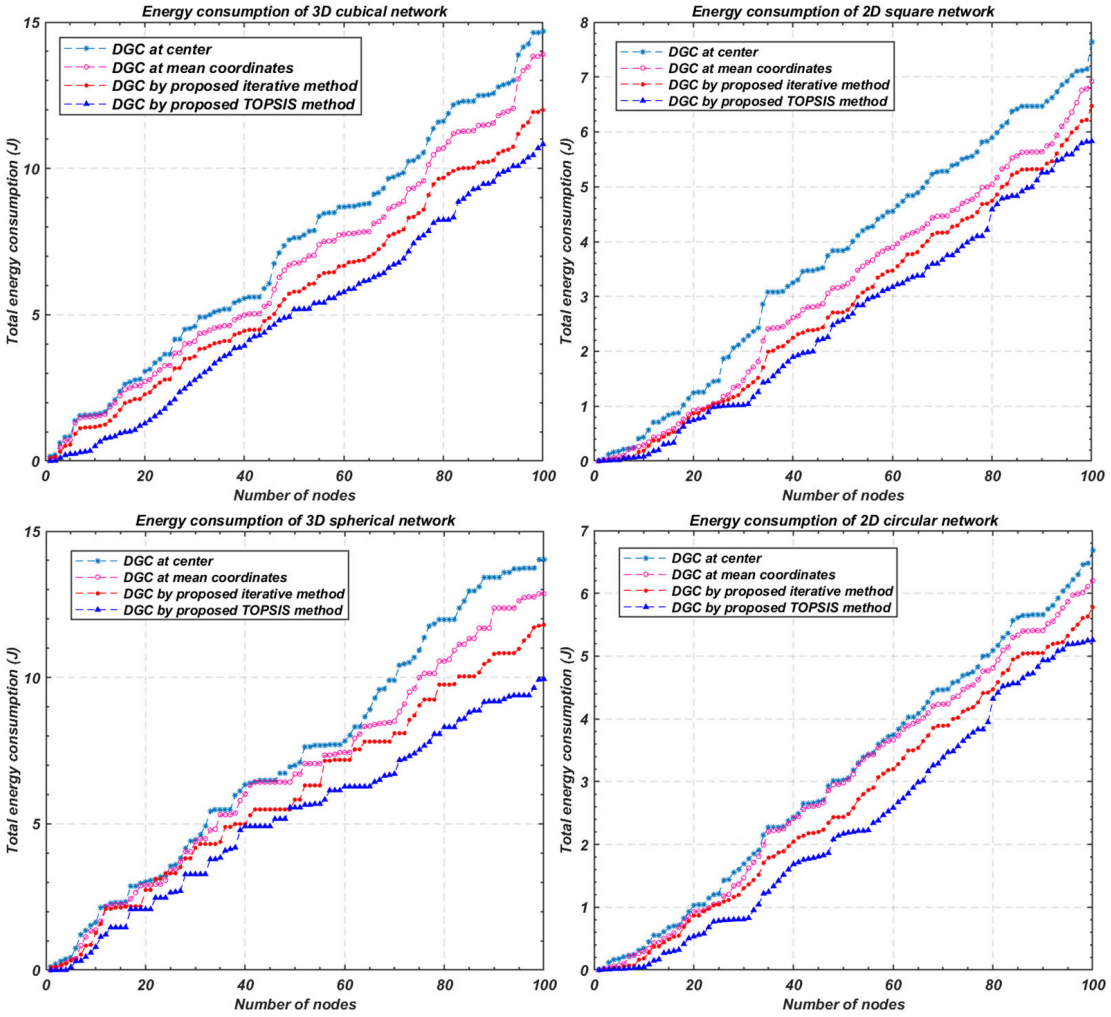

FIGURE 10. Total energy consumption of network in each round (flat network).

TABLE 2. Summary of total energy consumption in each round (flat network).

Network shape	DGC at center	DGC at mean coordinates	DGC by proposed iterative method	DGC by proposed TOPSIS based method
3D Cube	14.7	13.90	12.00	10.83
2D Square	7.64	6.92	6.47	5.83
3D Sphere	14.02	12.86	11.80	9.94
2D Circle	6.68	6.20	5.78	5.26

in terms of various QoS parameters. Following evaluation indicators have been used to analyze the performance of proposed techniques: network lifetime, energy consumption, balanced network operation, scalability, and adaptability. Table 1 shows the list of simulation parameters throughout the experiments.

A. ENERGY EFFICIENT DEPLOYMENT OF DGC

To evaluate the performance of energy efficient data gathering center (DGC) deployment, simulation experiments have been carried out in MATLAB. Simulation parameters have been shown in Table 1. To verify adaptability of the proposed deployment schemes the experiments have been conducted in four network shapes. Total energy consumption of the network during each round of operation is computed for the proposed deployment schemes. The results from proposed schemes are compared with the total energy consumption of network during each round when DGC is deployed at center of the network as well as when deployed at the mean location. To confirm the reliability of proposed schemes, Figures 10 and 11 correspond to the results of total energy

TABLE 3. Summary of total energy consumption in each round (clustered network).

Network shape	DGC at center	DGC at mean coordinates	DGC by proposed iterative method	DGC by proposed TOPSIS based method
3D Cube	1.13	1.08	1.05	1.05
2D Square	0.48	0.45	0.39	0.37
3D Sphere	1.12	0.91	0.85	0.81
2D Circle	0.44	0.43	0.41	0.41

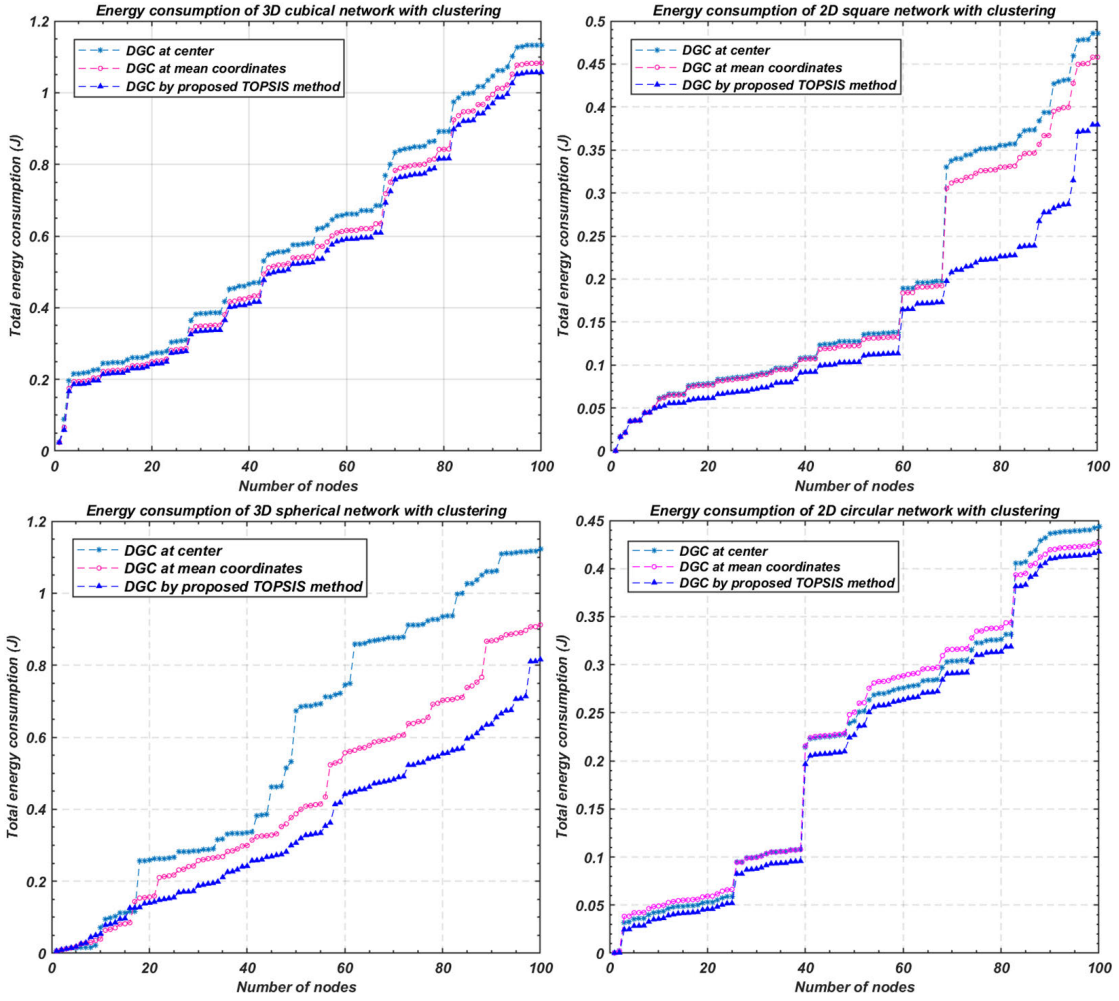

FIGURE 11. Total energy consumption of network in each round (clustered network).

TABLE 4. Comparison of state of the total energy consumption of STATE-OF-THE-ART sink deployment methods.

Nodes	PSO[71]	FPA[72]	GWO[73]	SCA[74]	MVO[75]	WOA[76]	HHO[69]	Proposed iterative method	Proposed TOPSIS method
100	36911	38537	36446	34920	35820	39222	34101	19465	18056
200	60637	60957	67000	73931	79044	80569	51805	22163	13360
300	88115	87028	83732	100829	113868	123869	60224	47913	26462
400	98697	191788	94931	114198	260659	270659	66005	65439	56661
500	105190	109630	120544	121820	392475	402475	70233	53150	49022
1000	131419	165651	133185	209715	468689	488989	107456	85443	77260
2000	198464	194892	188526	236876	591674	601674	124777	109121	95262
3000	247826	279863	223074	313128	643032	693089	150659	127200	101427
4000	267899	289874	244088	349696	665284	764098	160659	151362	112426
5000	298755	299995	267896	389654	699978	834058	180999	175727	131303

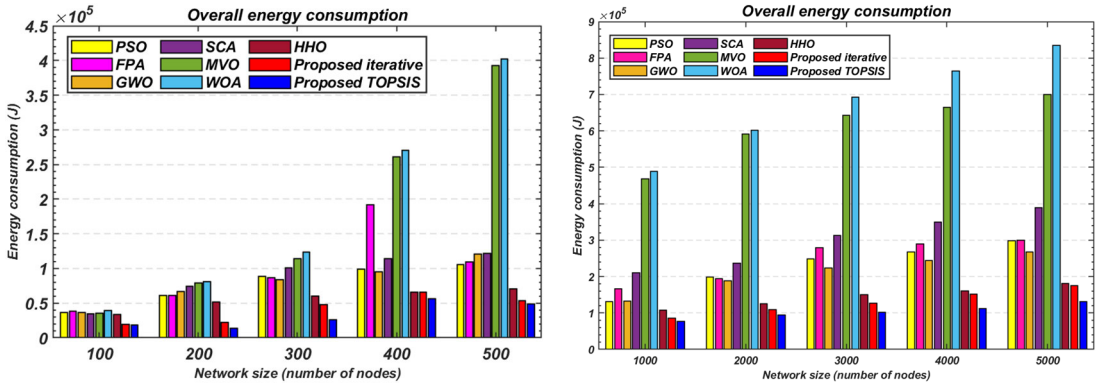

FIGURE 12. Comparison of overall energy consumption of different sink node deployment algorithms.

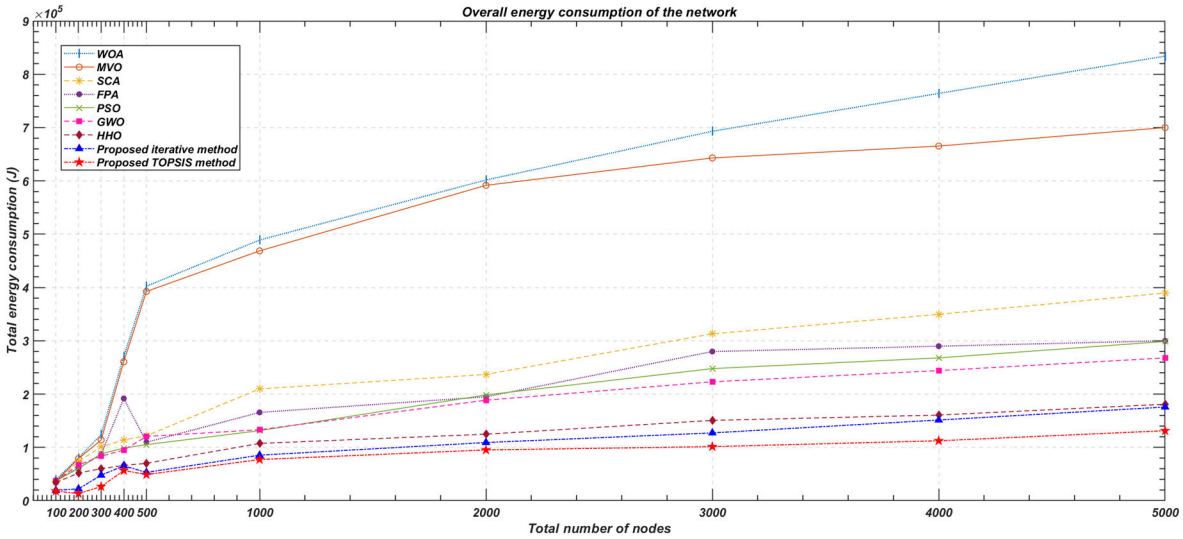

FIGURE 13. Overall energy consumption of varying network sizes.

consumption during one round of operation in the network with direct communication to the DGC and with multi-hop communication to DGC through cluster heads using k-means clustering. In each network geometry the proposed TOPSIS based deployment results in energy savings as compared to traditional deployment i.e., DGC at center and DGC at mean coordinates.

Network with hierarchical communication using k-means clustering consumes a lot less energy as compared to that with direct communication. Table 2 and 3 summarize the results of Figure 10 and 11. Proposed iterative method demonstrates a minimum and maximum of 2.78% and 24.12% decrease in total energy consumption. Whereas proposed TOPSIS based deployment method shows a minimum of 4.65% and maximum of 29.1% decrease in total energy consumption. Table 3 confirms that due to small energy consumption in clustered communication proposed iterative and proposed TOPSIS based deployment produce almost similar results.

The performance of proposed methods has been compared against seven well-known algorithms, such as PSO [71], FPA [72], GWO [73], SCA [74], MVO [75], WOA [76], and HHO [69]. The proposed methods have been tested in 10 different network sizes based on number of nodes. The results are compared with the power consumption of counterpart DGC deployment algorithms. In this experiment the overall energy consumption of all the algorithms is captured in a fixed number of iterations. Table 4 shows the total energy consumption for nine algorithms with respect to each size of the network. This is obvious from table 4 that proposed iterative method onsumes less overall energy compared to eight other methods whereas proposed TOPSIS method consumes least overall energy consumption in each scenario of network size. Figure 12 shows consistent decrease in energy consumption of proposed methods against seven methods in varying network sizes.

Figure 13 shows comparison of seven different deployment methods against two proposed methods graphically. It can be clearly seen that proposed iterative and TOPSIS methods demonstrate reduction in energy consumption consistently with each network size.

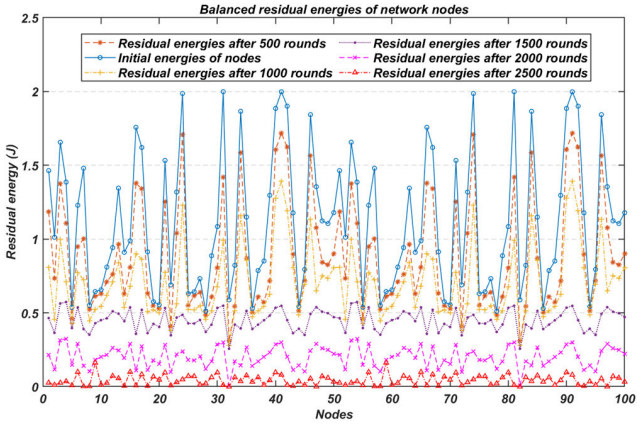

FIGURE 14. Balanced residual energies of devices.

Simulation experiments confirm that proposed TOPSIS based deployment of DGC outperforms not only traditional deployment schemes i.e., DGC at center and DGC at mean coordinates but also seven well-known deployment methods. It can be concluded from experiments that the results are consistent and reliable for each network shape considered and are also valid for both direct and clustered communication.

B. BALANCED ENERGY OPERATION OF NETWORK

In this work residual energies of the devices are aimed to be balanced with the network operation, while keeping the overall energy consumption minimum. Figure 14 demonstrates the range of device residual energies with the network operation, using proposed unequal clustering. The difference in energies was initially high. The difference of residual energies minimizes with increase in rounds of operation and therefore confirms the balanced operation of proposed unequal clustering. This result has been taken from the simulation of a cubical shape network of $100 \times 100 \times 100\ m^3$ dimensions.

For a spherical segmentation and unequal clustering using the proposed algorithm 4, balanced operation of both normal nodes and cluster heads has been shown in Figure 15. It can be seen that difference in energy consumption of each type of nodes is almost smooth.

C. AVERAGE RESIDUAL ENERGY

The aim of this experiment is to demonstrate performance of proposed method in terms of residual energy of the network in comparison to other state-of-the-art methods. This section shows achievements of proposed adaptive clustering method of algorithm 5 independently. For comparison with state-of-the-art Fuzzy Logic based unequal clustering [77] and other important LEACH based clustering methods, the proposed method is tested in a similar simulation set up. 1000 devices are deployed in a 1000m*1000m monitoring area and initial energy of the devices is kept fixed (0.5J) for this experiment.

Figure 16 shows the results of average residual energy of nodes after the network has executed 50, 100, and 150 rounds.

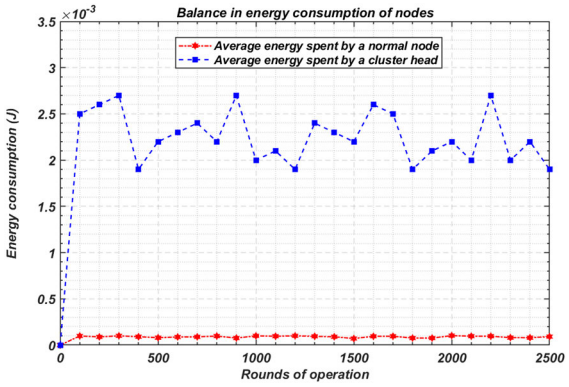

FIGURE 15. Average energy consumption of the devices.

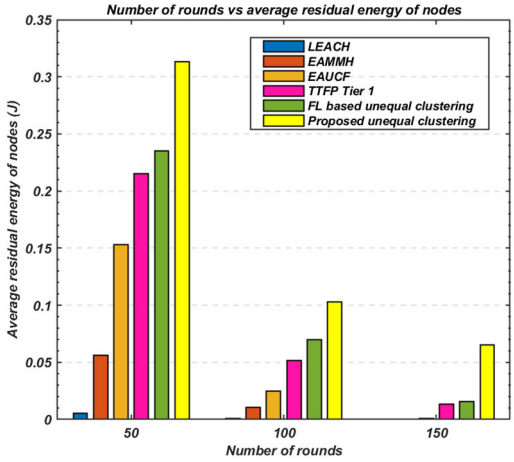

FIGURE 16. Average residual energies of devices.

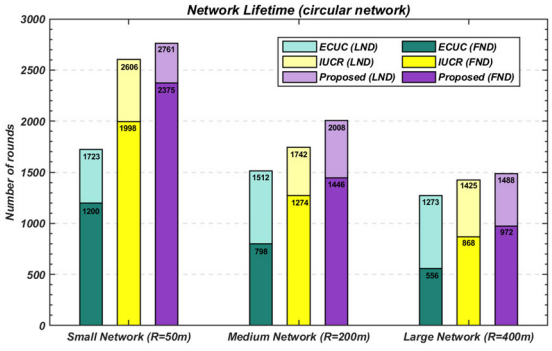

FIGURE 17. Network lifetime in different scale circular networks.

The bar chart in Figure 16 confirms that proposed algorithm is always higher than other algorithms in large scale deployment.

D. SCALABILITY AND IMPROVED LIFETIME

This section establishes a comparison of the proposed adaptive clustering described in algorithm 5 with the existing unequal clustering methods found in literature. Although there is lack of adaptive network shape independent clustering and routing protocols. Improved Unequal Clustering

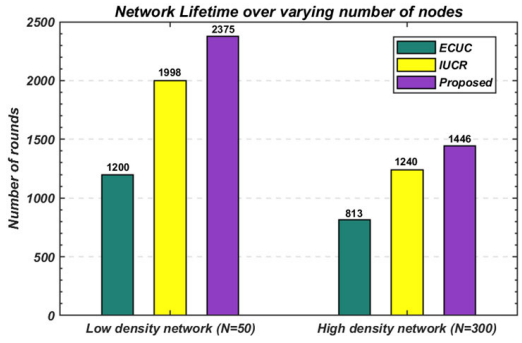

FIGURE 18. Network lifetime under different device densities.

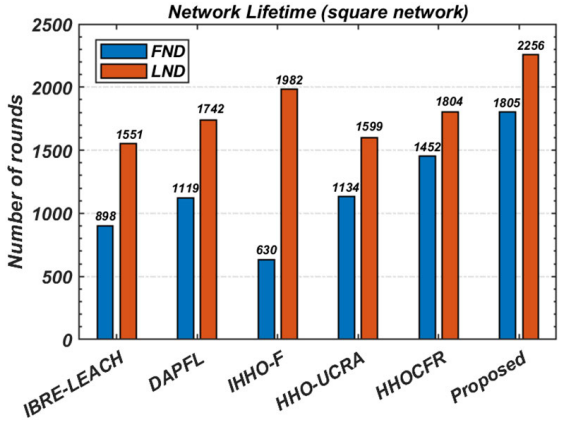

FIGURE 19. Network lifetime in different scale square networks.

Routing (IUCR) [78] and Energy efficient and Coverage-guaranteed Unequal-size Clustering (ECUC) [27] are recent unequal clustering methods for circular shape network. Measurements are taken to reveal how proposed method not only increases network lifetime on the first node death (FND), half node death (HND), and last node death (LND) scales, but also confirm the results are consistent for different sizes of the network. Figure 17 shows comparison of network lifetime achieved by proposed algorithm as compared to IUCR and ECUC. The simulation results in Figure 17, inform that the proposed adaptive unequal clustering method consistently outperforms both IUCR and ECUC on all network lifetime scales and across varying network sizes.

Furthermore, the proposed method also demonstrates stability in the achievements with different levels of node density as compared to IUCR and ECUC as shown in Figure 18. Proposed method shows superior performance within a small-scale network with 50 devices and achieves almost 45% and 12% improvement in network lifetime as compared to ECUC and IUCR respectively. These results are consistent for a large-scale network of 300 devices demonstrating 46% and 10.7% gain in network lifetime against ECUC and IUCR respectively.

In addition to unequal clustering methods for circular shape networks, recently many Harris Hawk Optimization and Fuzzy Logic based techniques have been used to optimize

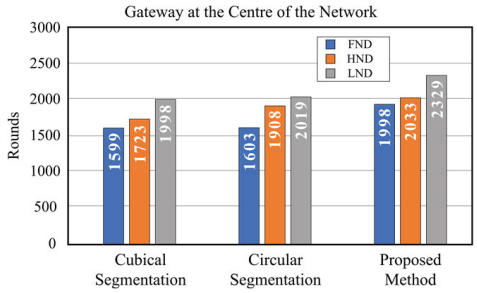

FIGURE 20. Comparison of network lifetime in fixed segmentations against proposed shape independent unequal clustering method with gateway at the center of the network.

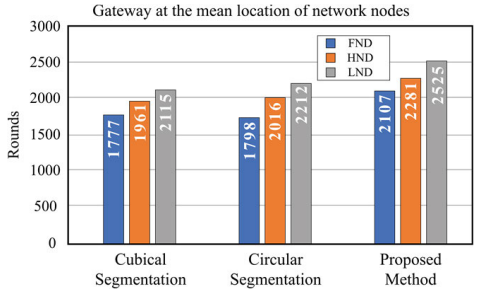

FIGURE 21. Comparison of network lifetime in two fixed segmentations against proposed adaptive unequal clustering method when DGC is at the mean location of the network.

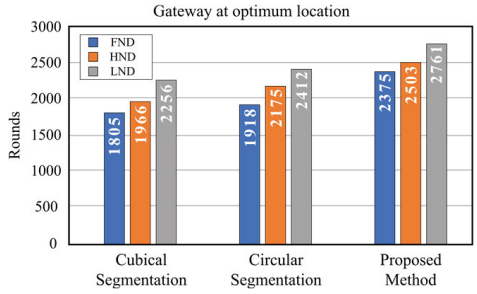

FIGURE 22. Comparison of network lifetime in fixed segmentations against proposed shape independent unequal clustering with gateway at TOPSIS based optimum location.

the performance of unequal clustering methods for square shape networks. To demonstrate the adaptability of proposed unequal clustering in shape varying networks, the network lifetime of proposed method is also compared against state-of-the-art techniques for square shape networks. The results in Figure 19 show network lifetime of proposed method against Harris Harks Optimization Clustering with Fuzzy Routing (HHOCFR) [79], Harris Hawk Optimization based Unequal Clustering Routing Algorithm (HHO-UCRA) [80], Improved Harris Hawk Algorithm with Fuzzy (IHHO-F) [81], Distributed clustering routing protocol combined Affinity Propagation with Fuzzy Logic (DAPFL) [82], and Improved Balanced Residual Energy LEACH, (IBRE-LEACH) [83].

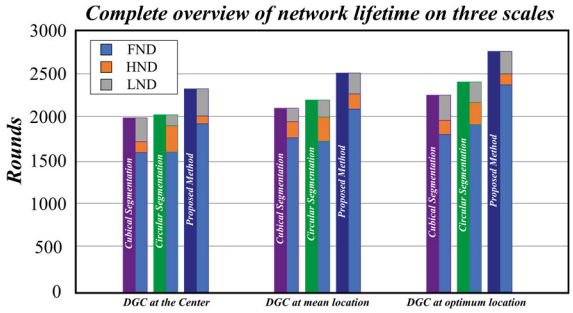

FIGURE 23. Summary of results with fixed shape segmentations and shape independent unequal clustering.

The results in Figure 19, confirm that the proposed method demonstrate 101%, 61% 186%, 59% and 24% increase in network lifetime on FND scale and 45%, 29%, 13%, 41% and 23% increase on LND scale as compared to IBRE-LEACH, DAPFL, IHHO-F, HHO-UCRA, and HHOCFR respectively.

E. ADAPTIVITY

In this section a comparison of shape specific 3D unequal clustering schemes of algorithm 3 and 4 has been presented against shape independent unequal clustering method of algorithm 5. The comparison has also been evaluated against all different deployment cases considered in algorithm 2. Results in Figures 20-23 show different scenarios to discover adaptability of the proposed methods. All three methods i.e., cubical segmentation, spherical segmentation and shape independent adaptive unequal clustering are evaluated in terms of network lifetime for three deployment cases of DGC. Results demonstrate that the increase in network lifetime is stable through different cases and best achievement is when TOPSIS based deployment of DGC is used with shape independent adaptive unequal clustering.

Figures 20-22 show gain in network lifetime on three scales: First Node Dead (FND), Half Nodes Dead (HND), and Last Node Dead (LND). Proposed adaptive unequal clustering demonstrates better performance as compared to cubical and spherical segmentation schemes due to the shape specific divisions.

Figure 20 shows when DGC is deployed at the center of the network regardless of the distribution of energies and data rate among devices, the cubical segmentation reaches 1599 round when the first node dies, 1723 round when half of the nodes are dead and 1998 rounds when all the devices have zero residual energy. Circular segmentation performs relatively better and shows that first node dies in 1603rd round and last node dies in 2019th round of network operation, whereas adaptive unequal clustering demonstrates a significant rise in network lifetime such that first node dies in 1998th round, which is when all the nodes would have died in cubical segmentation. It reaches 2329 rounds of operation to have network completely dis-functional. Figures 21 and 22 confirm similar results when DGC is placed at the mean coordinates and TOPSIS based optimum locations, respectively.

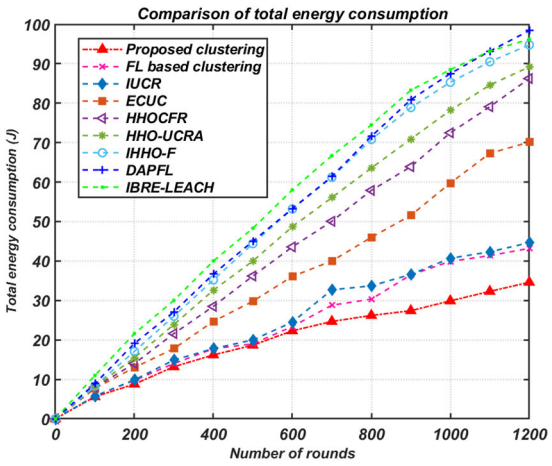

FIGURE 24. Overall energy consumption of the network.

Figure 23 summarizes the results of Figures 20-22 and demonstrates consistency and adaptability of the adaptive unequal clustering. It is observed that the network lifetime enhances by 32% and 27% with shape independent unequal clustering and optimum DGC deployment as compared to cubical and spherical segmentation based traditional unequal clustering respectively.

F. OVERALL ENERGY CONSUMPTION

In this section a comparison of overall energy consumption in proposed method has been developed with IBRE-LEACH [83], DAPFL [82], IHHO-F [81], HHO-UCRA [80], and HHOCFR [79], Fuzzy Logic based unequal clustering [77], IUCR [78], and ECUC [27]. Results demonstrate that after 1200 rounds of operation there is around 12.8%, 16.2%, 39.6%, 48.9%, 53.1%, 56.7%, 58.3%, and 61.4% decrease in overall energy consumption by using the proposed method as compared to FL based clustering, IUCR, ECUC, HHOCFR, HHO-UCRA, IHHO-F, DAPFL, and IBRE-LEACH respectively.

VIII. CONCLUSION

Cooperative operations in modern infrastructures such as Smart Cities and Internet of Things result in a huge number of interconnected devices as high as 4.1B. An energy balanced operation of devices with increased overall network lifetime using hierarchical routing has been explored. Firstly, an optimum deployment location of data gathering center using an iterative method and then using TOPSIS have been proposed. Then two fixed shape 3D network segmentation based unequal clustering schemes, namely cubical and spherical segmentations have been proposed. Finally, a shape independent adaptive unequal clustering technique has been developed. The results demonstrate that the proposed unequal clustering technique results in significant reduction of overall network energy consumption as compared to state-of-the-art methods. The decrease in energy consumption ranges from up to 12.8% as compared to FL based clustering to 61.4%

that in IBRE-LEACH. It is also concluded that the proposed schemes demonstrate consistent results in varying network sizes and device densities and are also adaptable to various 2D and 3D shape networks. In future it is intended to explore performance of proposed techniques with varying levels of device mobility.

REFERENCES

[1] Y.-D. Yao, X. Li, Y.-P. Cui, L. Deng, and C. Wang, "Game theory and coverage optimization based multihop routing protocol for network lifetime in wireless sensor networks," *IEEE Sensors J.*, vol. 22, no. 13, pp. 13739–13752, Jul. 2022, doi: 10.1109/JSEN.2022.3178441.

[2] M. Majid, S. Habib, A. R. Javed, M. Rizwan, G. Srivastava, T. R. Gadekallu, and J. C.-W. Lin, "Applications of wireless sensor networks and Internet of Things frameworks in the industry revolution 4.0: A systematic literature review," *Sensors*, vol. 22, no. 6, p. 2087, Mar. 2022, doi: 10.3390/s22062087.

[3] A. Sestino, M. I. Prete, L. Piper, and G. Guido, "Internet of Things and big data as enablers for business digitalization strategies," *Technovation*, vol. 98, Dec. 2020, Art. no. 102173, doi: 10.1016/j.technovation.2020.102173.

[4] Ericsson, Stockholm, Sweden. (2022). *Ericsson Mobility Report June 2022*. [Online]. Available: https://www.ericsson.com/49d3a0/assets/local/reports-papers/mobility-report/documents/2022/ericsson-mobilityreport-june-2022.pdf

[5] E. Estopace. *IDC Forecasts Connected IoT Devices to Generate 79.4ZB of Data in 2025*. FutureIoT. Accessed: Jun. 17, 2023. [Online]. Available: https://futureiot.tech/idc-forecasts-connected-iot-devices-to-generate-79-4zb-of-data-in-2025/

[6] D. Gariba and B. Pipaliya, "Modelling human behaviour in smart home energy management systems via machine learning techniques," in *Proc. Int. Autom. Control Conf. (CACS)*, Nov. 2016, pp. 53–58, doi: 10.1109/CACS.2016.7973883.

[7] R. Gantassi, Z. Masood, and Y. Choi, "Enhancing QoS and residual energy by using of grid-size clustering, k-means, and TSP algorithms with MDC in LEACH protocol," *IEEE Access*, vol. 10, pp. 58199–58211, 2022, doi: 10.1109/ACCESS.2022.3178434.

[8] B. B. Gouissem, R. Gantassi, and S. Hasnaoui, "Energy efficient grid based k-means clustering algorithm for large scale wireless sensor networks," *Int. J. Commun. Syst.*, vol. 35, no. 14, p. e5255, Sep. 2022, doi: 10.1002/dac.5255.

[9] R. Gantassi, B. Ben Gouissem, O. Cheikhrouhou, S. El Khediri, and S. Hasnaoui, "Optimizing quality of service of clustering protocols in large-scale wireless sensor networks with mobile data collector and machine learning," *Secur. Commun. Netw.*, vol. 2021, pp. 1–12, Mar. 2021, doi: 10.1155/2021/5531185.

[10] S. Sasirekha and S. Swamynathan, "Cluster-chain mobile agent routing algorithm for efficient data aggregation in wireless sensor network," *J. Commun. Netw.*, vol. 19, no. 4, pp. 392–401, Aug. 2017.

[11] N. Sharmin, A. Karmaker, W. L. Lambert, M. S. Alam, and M. S. A. Shawkat, "Minimizing the energy hole problem in wireless sensor networks: A wedge merging approach," *Sensors*, vol. 20, no. 1, p. 277, Jan. 2020, doi: 10.3390/s20010277.

[12] D. Sethi, "An approach to optimize homogeneous and heterogeneous routing protocols in WSN using sink mobility," *MAPAN*, vol. 35, no. 2, pp. 241–250, Jun. 2020, doi: 10.1007/s12647-020-00366-5.

[13] A. Shukla and S. Tripathi, "An effective relay node selection technique for energy efficient WSN-assisted IoT," *Wireless Pers. Commun.*, vol. 112, no. 4, pp. 2611–2641, Jun. 2020, doi: 10.1007/s11277-020-07167-8.

[14] N. N. Dezfouli and H. Barati, "A distributed energy-efficient approach for hole repair in wireless sensor networks," *Wireless Netw.*, vol. 26, no. 3, pp. 1839–1855, Apr. 2020, doi: 10.1007/s11276-018-1867-0.

[15] R. Mishra, V. Jha, R. K. Tripathi, and A. K. Sharma, "Corona based node distribution scheme targeting energy balancing in wireless sensor networks for the sensors having limited sensing range," *Wireless Netw.*, vol. 26, no. 2, pp. 879–896, Feb. 2020, doi: 10.1007/s11276-018-1834-9.

[16] E. F. A. Elsmany, M. A. Omar, T.-C. Wan, and A. A. Altahir, "EESRA: Energy efficient scalable routing algorithm for wireless sensor networks," *IEEE Access*, vol. 7, pp. 96974–96983, 2019, doi: 10.1109/ACCESS.2019.2929578.

[17] S. Chowdhury and C. Giri, "Energy and network balanced distributed clustering in wireless sensor network," *Wireless Pers. Commun.*, vol. 105, no. 3, pp. 1083–1109, Apr. 2019, doi: 10.1007/s11277-019-06137-z.

[18] N. Jan, A. R. Hameed, B. Ali, R. Ullah, K. Ullah, and N. Javaid, "A wireless sensor networks balanced energy consumption protocol," in *Proc. 31st Int. Conf. Adv. Inf. Netw. Appl. Workshops (WAINA)*, Mar. 2017, pp. 730–736, doi: 10.1109/WAINA.2017.122.

[19] C. Sha, C. Ren, R. Malekian, M. Wu, H. Huang, and N. Ye, "A type of virtual force-based energy-hole mitigation strategy for sensor networks," *IEEE Sensors J.*, vol. 20, no. 2, pp. 1105–1119, Jan. 2020, doi: 10.1109/JSEN.2019.2945595.

[20] S. Kumar, P. R. Gautam, A. Verma, R. Verma, and A. Kumar, "Energy efficient routing using sectors based energy-hole reduction in WSNs," in *Proc. Int. Conf. Electr., Electron. Comput. Eng. (UPCON)*, Nov. 2019, pp. 1–4, doi: 10.1109/UPCON47278.2019.8980254.

[21] N. Jan, N. Javaid, Q. Javaid, N. Alrajeh, M. Alam, Z. A. Khan, and I. A. Niaz, "A balanced energy-consuming and hole-alleviating algorithm for wireless sensor networks," *IEEE Access*, vol. 5, pp. 6134–6150, 2017.

[22] X. Zhao, X. Xiong, Z. Sun, X. Zhang, and Z. Sun, "An immune clone selection based power control strategy for alleviating energy hole problems in wireless sensor networks," *J. Ambient Intell. Humanized Comput.*, vol. 11, no. 6, pp. 2505–2518, Jun. 2020, doi: 10.1007/s12652-019-01300-7.

[23] N. Javaid, T. Hafeez, Z. Wadud, N. Alrajeh, M. S. Alabed, and N. Guizani, "Establishing a cooperation-based and void node avoiding energy-efficient underwater WSN for a cloud," *IEEE Access*, vol. 5, pp. 11582–11593, 2017, doi: 10.1109/ACCESS.2017.2707531.

[24] I. S. Akila and R. Venkatesan, "An energy balanced geo-cluster head set based multi-hop routing for wireless sensor networks," *Cluster Comput.*, vol. 22, no. 4, pp. 9865–9874, Jul. 2019, doi: 10.1007/s10586-018-1724-z.

[25] A. Lipare, D. R. Edla, and R. Dharavath, "Energy efficient routing structure to avoid energy hole problem in multi-layer network model," *Wireless Pers. Commun.*, vol. 112, no. 4, pp. 2575–2596, Jun. 2020, doi: 10.1007/s11277-020-07165-w.

[26] Z. Wadud, N. Javaid, M. Khan, N. Alrajeh, M. Alabed, and N. Guizani, "Lifetime maximization via hole alleviation in IoT enabling heterogeneous wireless sensor networks," *Sensors*, vol. 17, no. 7, p. 1677, Jul. 2017, doi: 10.3390/s17071677.

[27] N. Gharaei, Y. D. Al-Otaibi, S. A. Butt, G. Sahar, and S. Rahim, "Energy-efficient and coverage-guaranteed unequal-sized clustering for wireless sensor networks," *IEEE Access*, vol. 7, pp. 157883–157891, 2019, doi: 10.1109/ACCESS.2019.2950237.

[28] R. Yarinezhad and A. Sarabi, "Reducing delay and energy consumption in wireless sensor networks by making virtual grid infrastructure and using mobile sink," *Int. J. Electron. Commun.*, vol. 84, pp. 144–152, Feb. 2018.

[29] I. Azam, N. Javaid, A. Ahmad, W. Abdul, A. Almogren, and A. Alamri, "Balanced load distribution with energy hole avoidance in underwater WSNs," *IEEE Access*, vol. 5, pp. 15206–15221, 2017, doi: 10.1109/ACCESS.2017.2660767.

[30] X. Liu and P. Zhang, "Data drainage: A novel load balancing strategy for wireless sensor networks," *IEEE Commun. Lett.*, vol. 22, no. 1, pp. 125–128, Jan. 2018, doi: 10.1109/LCOMM.2017.2751601.

[31] N. Gharaei, K. A. Bakar, S. M. Hashim, A. H. Pourasl, M. Siraj, and T. Darwish, "An energy-efficient mobile sink-based unequal clustering mechanism for WSNs," *Sensors*, vol. 17, no. 8, p. 1858, Aug. 2017, doi: 10.3390/s17081858.

[32] X. Liu, "An optimal-distance-based transmission strategy for lifetime maximization of wireless sensor networks," *IEEE Sensors J.*, vol. 15, no. 6, pp. 3484–3491, Jun. 2015, doi: 10.1109/JSEN.2014.2372340.

[33] A. Lipare, D. R. Edla, and V. Kuppili, "Energy efficient load balancing approach for avoiding energy hole problem in WSN using grey wolf optimizer with novel fitness function," *Appl. Soft Comput.*, vol. 84, Nov. 2019, Art. no. 105706, doi: 10.1016/j.asoc.2019.105706.

[34] N. M. Shagari, M. Y. I. Idris, R. B. Salleh, I. Ahmedy, G. Murtaza, and H. A. Shehadeh, "Heterogeneous energy and traffic aware sleep-awake cluster-based routing protocol for wireless sensor network," *IEEE Access*, vol. 8, pp. 12232–12252, 2020.

[35] L. Yang, Y. Lu, L. Xiong, Y. Tao, and Y. Zhong, "A game theoretic approach for balancing energy consumption in clustered wireless sensor networks," *Sensors*, vol. 17, no. 11, p. 2654, Nov. 2017, doi: 10.3390/s17112654.

[36] Y. Zhang, X. Zhang, S. Ning, J. Gao, and Y. Liu, "Energy-efficient multilevel heterogeneous routing protocol for wireless sensor networks," *IEEE Access*, vol. 7, pp. 55873–55884, 2019, doi: 10.1109/ACCESS.2019.2900742.

[37] C. Gherbi, Z. Aliouat, and M. Benmohammed, "A novel load balancing scheduling algorithm for wireless sensor networks," *J. Netw. Syst. Manage.*, vol. 27, no. 2, pp. 430–462, Apr. 2019, doi: 10.1007/s10922-018-9473-0.

[38] S. Zakariayi and S. Babaie, "DEHCIC: A distributed energy-aware hexagon based clustering algorithm to improve coverage in wireless sensor networks," *Peer-to-Peer Netw. Appl.*, vol. 12, no. 4, pp. 689–704, Jul. 2019, doi: 10.1007/s12083-018-0666-9.

[39] V. Nehra, A. K. Sharma, and R. K. Tripathi, "I-DEEC: Improved DEEC for blanket coverage in heterogeneous wireless sensor networks," *J. Ambient Intell. Humanized Comput.*, vol. 11, no. 9, pp. 3687–3698, Sep. 2020, doi: 10.1007/s12652-019-01552-3.

[40] Y. Xue, X. Chang, S. Zhong, and Y. Zhuang, "An efficient energy hole alleviating algorithm for wireless sensor networks," *IEEE Trans. Consum. Electron.*, vol. 60, no. 3, pp. 347–355, Aug. 2014.

[41] K. Koosheshi and S. Ebadi, "Optimization energy consumption with multiple mobile sinks using fuzzy logic in wireless sensor networks," *Wireless Netw.*, vol. 25, no. 3, pp. 1215–1234, Apr. 2019, doi: 10.1007/s11276-018-1715-2.

[42] S. Mostafavi and V. Hakami, "A new rank-order clustering algorithm for prolonging the lifetime of wireless sensor networks," *Int. J. Commun. Syst.*, vol. 33, no. 7, p. e4313, May 2020, doi: 10.1002/dac.4313.

[43] J. Wang, Y. Gao, K. Wang, A. Sangaiah, and S.-J. Lim, "An affinity propagation-based self-adaptive clustering method for wireless sensor networks," *Sensors*, vol. 19, no. 11, p. 2579, Jun. 2019, doi: 10.3390/s19112579.

[44] R. Vishnuvarthan, R. Sakthivel, V. Bhanumathi, and K. Muralitharan, "Energy-efficient data collection in strip-based wireless sensor networks with optimal speed mobile data collectors," *Comput. Netw.*, vol. 156, pp. 33–40, Jun. 2019, doi: 10.1016/j.comnet.2019.03.019.

[45] R. Elkamel, A. Messouadi, and A. Cherif, "Extending the lifetime of wireless sensor networks through mitigating the hot spot problem," *J. Parallel Distrib. Comput.*, vol. 133, pp. 159–169, Nov. 2019, doi: 10.1016/j.jpdc.2019.06.007.

[46] K. Sundaran, V. Ganapathy, and P. Sudhakara, "Energy minimization in wireless sensor networks by incorporating unequal clusters in multi-sector environment," *Cluster Comput.*, vol. 22, no. 4, pp. 9599–9613, Jul. 2019, doi: 10.1007/s10586-017-1279-4.

[47] S. Tanessakulwattana and C. Pornavalai, "Multipath energy balancing for clustered wireless sensor networks," *Wireless Netw.*, vol. 25, no. 5, pp. 2537–2558, Jul. 2019, doi: 10.1007/s11276-018-1684-5.

[48] F. Entezami and C. Politis, "Three-dimensional position-based adaptive real-time routing protocol for wireless sensor networks," *EURASIP J. Wireless Commun. Netw.*, vol. 2015, no. 1, p. 197, Dec. 2015, doi: 10.1186/s13638-015-0419-x.

[49] A. Ghosal and S. Halder, "Lifetime optimizing clustering structure using Archimedes' spiral-based deployment in WSNs," *IEEE Syst. J.*, vol. 11, no. 2, pp. 1039–1048, Jun. 2017, doi: 10.1109/JSYST.2015.2434498.

[50] Y. Xu, W. Jiao, and M. Tian, "An energy-efficient routing protocol for 3D wireless sensor networks," *IEEE Sensors J.*, vol. 21, no. 17, pp. 19550–19559, Sep. 2021, doi: 10.1109/JSEN.2021.3086806.

[51] L. D. Xu, W. He, and S. Li, "Internet of Things in industries: A survey," *IEEE Trans. Ind. Informat.*, vol. 10, no. 4, pp. 2233–2243, Nov. 2014, doi: 10.1109/TII.2014.2300753.

[52] M. Getahun, M. Azath, D. P. Sharma, A. Tuni, and A. Adane, "Efficient energy utilization algorithm through energy harvesting for heterogeneous clustered wireless sensor network," *Wireless Commun. Mobile Comput.*, vol. 2022, Apr. 2022, Art. no. e4154742, doi: 10.1155/2022/4154742.

[53] Z. Wang, L. Shao, S. Yang, and J. Wang, "LEMH: Low-energy-first electoral multipath alternating multihop routing algorithm for wireless sensor networks," *IEEE Sensors J.*, vol. 22, no. 16, pp. 16687–16704, Aug. 2022, doi: 10.1109/JSEN.2022.3191321.

[54] T. Shafique, R. Gantassi, A.-H. Soliman, A. Amjad, Z.-Q. Hui, and Y. Choi, "A review of energy hole mitigating techniques in multi-hop many to one communication and its significance in IoT oriented smart city infrastructure," *IEEE Access*, vol. 11, pp. 121340–121367, 2023, doi: 10.1109/ACCESS.2023.3327311.

[55] Y. Yao, D. Xie, Y. Li, C. Wang, and Y. Li, "Routing protocol for wireless sensor networks based on archimedes optimization algorithm," *IEEE Sensors J.*, vol. 22, no. 15, pp. 15561–15573, Aug. 2022, doi: 10.1109/JSEN.2022.3186063.

[56] S. Yu, X. Liu, A. Liu, N. Xiong, Z. Cai, and T. Wang, "An adaption broadcast radius-based code dissemination scheme for low energy wireless sensor networks," *Sensors*, vol. 18, no. 5, p. 1509, May 2018, doi: 10.3390/s18051509.

[57] F. Ullah, M. Z. Khan, M. Faisal, H. U. Rehman, S. Abbas, and F. S. Mubarek, "An energy efficient and reliable routing scheme to enhance the stability period in wireless body area networks," *Comput. Commun.*, vol. 165, pp. 20–32, Jan. 2021, doi: 10.1016/j.comcom.2020.10.017.

[58] W. R. Heinzelman, A. Chandrakasan, and H. Balakrishnan, "Energy-efficient communication protocol for wireless microsensor networks," in *Proc. 33rd Annu. Hawaii Int. Conf. Syst. Sci.*, vol. 2, Jan. 2000, p. 10, doi: 10.1109/hicss.2000.926982.

[59] W. B. Heinzelman, A. P. Chandrakasan, and H. Balakrishnan, "An application-specific protocol architecture for wireless microsensor networks," *IEEE Trans. Wireless Commun.*, vol. 1, no. 4, pp. 660–670, Oct. 2002, doi: 10.1109/TWC.2002.804190.

[60] O. Younis and S. Fahmy, "HEED: A hybrid, energy-efficient, distributed clustering approach for ad hoc sensor networks," *IEEE Trans. Mobile Comput.*, vol. 3, no. 4, pp. 366–379, Dec. 2004, doi: 10.1109/TMC.2004.41.

[61] K. Du, J. Wu, and D. Zhou, "Chain-based protocols for data broadcasting and gathering in the sensor networks," in *Proc. Int. Parallel Distrib. Process. Symp.*, Apr. 2003, p. 8.

[62] G. J. Pottie and W. J. Kaiser, "Wireless integrated network sensors," *Commun. ACM*, vol. 43, no. 5, pp. 51–58, May 2000.

[63] F. Zhu and J. Wei, "An energy-efficient unequal clustering routing protocol for wireless sensor networks," *Int. J. Distrib. Sensor Netw.*, vol. 15, no. 9, Sep. 2019, Art. no. 155014771987938, doi: 10.1177/1550147719879384.

[64] S. M. M. H. Daneshvar, P. A. A. Mohajer, and S. M. Mazinani, "Energy-efficient routing in WSN: A centralized cluster-based approach via grey wolf optimizer," *IEEE Access*, vol. 7, pp. 170019–170031, 2019, doi: 10.1109/ACCESS.2019.2955993.

[65] S. M. M. H. Daneshvar and S. M. Mazinani, "On the best fitness function for the WSN lifetime maximization: A solution based on a modified salp swarm algorithm for centralized clustering and routing," *IEEE Trans. Netw. Service Manage.*, vol. 20, no. 4, pp. 4244–4254, Dec. 2023, doi: 10.1109/TNSM.2023.3283248.

[66] P. Chatterjee, S. C. Ghosh, and N. Das, "Load balanced coverage with graded node deployment in wireless sensor networks," *IEEE Trans. Multi-Scale Comput. Syst.*, vol. 3, no. 2, pp. 100–112, Apr. 2017, doi: 10.1109/TMSCS.2017.2672553.

[67] F. Chen and R. Li, "Single sink node placement strategy in wireless sensor networks," in *Proc. Int. Conf. Electric Inf. Control Eng.*, Wuhan, China, Apr. 2011, pp. 1700–1703, doi: 10.1109/ICEICE.2011.5778162.

[68] M. M. Ahmed, E. H. Houssein, A. E. Hassanien, A. Taha, and E. Hassanien, "Maximizing lifetime of wireless sensor networks based on whale optimization algorithm," in *Proc. Int. Conf. Adv. Intell. Syst. Inform.*, in Advances in Intelligent Systems and Computing, A. E. Hassanien, K. Shaalan, T. Gaber, and M. F. Tolba. Cham, Switzerland: Springer, 2017, pp. 724–733, doi: 10.1007/978-3-319-64861-3_68.

[69] E. H. Houssein, M. R. Saad, K. Hussain, W. Zhu, H. Shaban, and M. Hassaballah, "Optimal sink node placement in large scale wireless sensor networks based on Harris' hawk optimization algorithm," *IEEE Access*, vol. 8, pp. 19381–19397, 2020, doi: 10.1109/ACCESS.2020.2968981.

[70] L. Ren, Y. Zhang, Y. Wang, and Z. Sun, "Comparative analysis of a novel M-TOPSIS method and TOPSIS," *Appl. Math. Res. Exp.*, vol. 2007, 2007, Art. no. abm005.

[71] H. Banka and P. K. Jana, "PSO-based multiple-sink placement algorithm for protracting the lifetime of wireless sensor networks," in *Proc. 2nd Int. Conf. Comput. Commun. Technol.*, in Advances in Intelligent Systems and Computing, vol. 1, S. C. Satapathy, K. S. Raju, J. K. Mandal, and V. Bhateja, Eds. New Delhi, India: Springer, 2016, pp. 605–616, doi: 10.1007/978-81-322-2517-1_58.

[72] X.-S. Yang, "Flower pollination algorithm for global optimization," in *Unconventional Computation and Natural Computation* (Lecture Notes in Computer Science), J. Durand-Lose and N. Jonoska, Eds. Berlin, Germany: Springer, 2012, pp. 240–249, doi: 10.1007/978-3-642-32894-7_27.

[73] S. Mirjalili, S. M. Mirjalili, and A. Lewis, "Grey wolf optimizer," *Adv. Eng. Softw.*, vol. 69, pp. 46–61, Mar. 2014, doi: 10.1016/j.advengsoft.2013.12.007.
[74] S. Mirjalili, "SCA: A sine cosine algorithm for solving optimization problems," *Knowl.-Based Syst.*, vol. 96, pp. 120–133, Mar. 2016, doi: 10.1016/j.knosys.2015.12.022.
[75] S. Mirjalili, S. M. Mirjalili, and A. Hatamlou, "Multi-verse optimizer: A nature-inspired algorithm for global optimization," *Neural Comput. Appl.*, vol. 27, no. 2, pp. 495–513, Feb. 2016, doi: 10.1007/s00521-015-1870-7.
[76] S. Mirjalili and A. Lewis, "The whale optimization algorithm," *Adv. Eng. Softw.*, vol. 95, pp. 51–67, May 2016, doi: 10.1016/j.advengsoft.2016.01.008.
[77] M. Adnan, L. Yang, T. Ahmad, and Y. Tao, "An unequally clustered multi-hop routing protocol based on fuzzy logic for wireless sensor networks," *IEEE Access*, vol. 9, pp. 38531–38545, 2021, doi: 10.1109/ACCESS.2021.3063097.
[78] M. A. Alharbi and M. Kolberg, "Improved unequal-clustering and routing protocol," *IEEE Sensors J.*, vol. 21, no. 20, pp. 23711–23721, Oct. 2021, doi: 10.1109/JSEN.2021.3111698.
[79] D. Jing, "Harris harks optimization based clustering with fuzzy routing for lifetime enhancing in wireless sensor networks," *IEEE Access*, vol. 12, pp. 12149–12163, 2024, doi: 10.1109/ACCESS.2024.3354276.
[80] D. Jain, P. K. Shukla, and S. Varma, "Energy efficient architecture for mitigating the hot-spot problem in wireless sensor networks," *J. Ambient Intell. Humanized Comput.*, vol. 14, no. 8, pp. 10587–10604, Aug. 2023, doi: 10.1007/s12652-022-03711-5.
[81] V. Nivedhitha, P. Thirumurugan, A. G. Saminathan, and V. Eswaramoorthy, "Combination of improved Harris's hawk optimization with fuzzy to improve clustering in wireless sensor network," *J. Intell. Fuzzy Syst.*, vol. 41, no. 6, pp. 5969–5984, Dec. 2021, doi: 10.3233/jifs-202098.
[82] C.-H. Wang, H.-S. Hu, Z.-G. Zhang, Y.-X. Guo, and J.-F. Zhang, "Distributed energy-efficient clustering routing protocol for wireless sensor networks using affinity propagation and fuzzy logic," *Soft Comput.*, vol. 26, no. 15, pp. 7143–7158, Aug. 2022, doi: 10.1007/s00500-022-07191-9.
[83] I. Daanoune and A. Baghdad, "IBRE-LEACH: Improving the performance of the BRE-LEACH for wireless sensor networks," *Wireless Pers. Commun.*, vol. 126, no. 4, pp. 3495–3513, Oct. 2022, doi: 10.1007/s11277-022-09876-8.

TAMOOR SHAFIQUE received the B.Sc. degree (Hons.) in electrical engineering from Mirpur University of Science and Technology (MUST), Mirpur, Azad Jammu & Kashmir, in 2010, and the M.Sc. degree in electrical engineering from the COMSATS Institute of Engineering and Technology, Islamabad, Pakistan, in 2013. He is currently a Senior Lecturer in automation and robotics engineering with Staffordshire University. His current research interests include resource constraints in smart cities, hostile wireless sensor networks, make-up invariant face recognition, and standardized routing protocols for the Internet of Things.

ABDEL-HAMID SOLIMAN has over 33 years of experience in the academic and industrial fields. He has a multi-disciplinary academic/research experience in digital signal processing, telecommunications, data acquisition systems, wireless sensor networks (WSN), the Internet of Things (IoT), fiber optics communication, and image/video processing. He is working to harness and integrate different technologies towards implementing smart systems to contribute to smart cities and real-life applications. His research activities are not limited to the national level within the U.K., but are internationally extended to many partner universities in various countries. His research has produced over 70 refereed articles. In addition to his research activities, he is involved in several enterprise projects and consultancy activities for national and international companies. Since 2007, he has been leading and involved in several externally funded projects on national, European, and international levels totaling more than £20M.

His work has been recognized through several awards, such as the Lord Stafford Award "Impact through Innovation," for designing and developing a smart monitoring and controlling system for diabetic people, the AWM ICT Excellence Awards for "Best Knowledge Transfer Project" category, for designing and developing an electronic bladder diary, and UHNS "Clinical Innovation" Award, for designing and developing an online multimedia-based training system for surgeons. He is an Associate Editor of IEEE ACCESS journal and a regular reviewer in several respected journals and conferences.

ANAS AMJAD received the B.Eng. (Hons.) and Ph.D. degrees from Staffordshire University, Stoke-on-Trent, U.K., in 2011 and 2017, respectively. He is currently the Course Director of Electrical and Electronic Engineering with Staffordshire University. His current research interests include resource optimization for the Internet of Things, data prioritization in smart cities, and quality assessment for the future generation of wireless networks.

Open Access funding provided by 'Staffordshire University' within the CRUI CARE Agreement